Pergamon

PII: S0277–3791(97)00099-1

Quaternary Science Reviews, Vol. 17, pp. 1185–1201, 1998

0277–3791/98/$–see front matter

TROPICAL SEA-SURFACE TEMPERATURES DURING THE LAST GLACIAL PERIOD: A VIEW BASED ON ALKENONES IN INDIAN OCEAN SEDIMENTS

CORINNE SONZOGNI, EDOUARD BARD and FRAUKE ROSTEK

CEREGE, CNRS-Université Aix-Marseille III, Europole de l'Arbois, BP 80, 13545 Aix-en-Provence cedex 4, France

(E-mail sonzogni@cerege.fr)

Abstract—The quantification of tropical temperatures during the last glacial cycle (0–150 kyr BP) is a controversial issue since different proxies seem to provide conflicting informations. To obtain a complementary point of view, we use the alkenone method to estimate sea-surface temperatures and focus our work on deep-sea sediments recovered from the tropical Indian Ocean. We present alkenone data obtained in two cores which cover in detail the last deglaciation and in about twenty cores distributed between 20°S and 20°N that were chosen to evaluate the temperature contrast of the last glacial-interglacial transition. Our results indicate that Indian Ocean tropical temperatures remained an average within 1.5–2.5°C of their present values during the last glaciation. At 10°N the last deglaciation is characterized by two warming steps which is similar to the classical deglacial chronology observed in the North Atlantic area. At 20°S the deglacial warming occurred at ca. 15 cal kyr BP, lagging significantly (5–4 kyr) behind the Antarctic warming, but in phase with northern hemisphere time series.

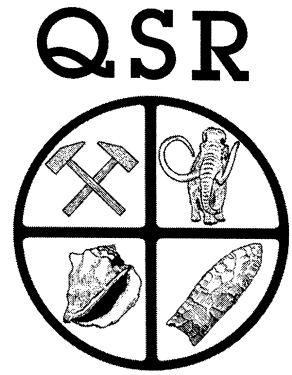

INTRODUCTION

Since the pioneering work by Webster and Streten (1978) and the general circulation modeling by Rind and Peteet (1985) it is recognized that there is a discrepancy between glacial temperature reconstructions based on terrestrial and oceanic evidences. Taken at face values these different studies would imply large gradients ($>5°C$) between oceanic and continental temperatures that are difficult to sustain based on general circulation models (Rind and Peteet, 1985). Broecker (1995) identified this problem as the top priority for the advancement of our understanding of past climatic change and of our quest to evaluate the potential impacts of the current greenhouse buildup.

Direct quantification of tropical temperatures comes from several proxies measured in different terrestrial and marine archives. Pollen species from peat bogs (Bonnefille *et al*., 1990, 1992), noble gas concentrations in water from deep aquifers (Stute *et al*., 1994) and isotopes in mountain glaciers (Thompson *et al*., 1995) indicate that glacial tropical temperatures were colder than today by about 3–4°C, 5–6°C and 7–8°C, respectively. The last two estimates are compatible with sea surface temperatures (SST) based on trace elements in scleratinian corals which suggest a glacial cooling on the order of 5–6°C (Beck *et al*., 1992; Guilderson *et al*., 1994; Min *et al*., 1995). However, these SSTs are in clear conflict with previous reconstructions based on foraminiferal transfer functions (TF) which indicate almost no cooling in the tropical belt during the last glacial maximum (LGM; CLIMAP, 1981). In addition, paleotemperatures estimated by the TF method (Imbrie and Kipp, 1971) have been confirmed through the use of the Modern Analogue Technique (MAT; Prell, 1985; Anderson *et al*., 1989; Thunell *et al*., 1994, Miao *et al*., 1994).

Temperatures based on the TF and MAT methods were verified independently by $\delta^{18}O$ measurements of planktonic foraminifera which averaged about 1.5‰ heavier during the LGM than today (Broecker, 1986). Subtracting a shift of about 1.25‰ (Fairbanks, 1989) or 1‰ (Schrag *et al*., 1996) attributable to sea-level variations leaves about 0.25 or 0.5‰ for temperature changes, equivalent to about 1 and 2°C and cooling in the tropical oceans. Bioturbation could have reduced the Glacial/Holocene $\delta^{18}O$ contrast of numerous records but several studies obtained on cores with high sedimentation rate (e.g. Linsley, 1996), or with low bioturbation rate (e.g. Crowley and Matthews, 1981) and $\delta^{18}O$ measurements on single planktonic foraminifera (Stott and Tang, 1996; Billups and Spero, 1996) demonstrate that this explanation does not hold and that the tropical cooling was indeed small ($<3°C$) during the last glacial maximum.

Averaging spatial features leads sometimes to oversimplification and several of the observed temperature differences could be due to regional responses to global cooling linked to circulation changes in the atmosphere and/or oceans. For example, a longitudinal

gradient is revealed by $\delta^{18}O$ analyses of planktonic foraminifera which suggests that tropical cooling in the Atlantic was more intense than in the Indian and Pacific oceans (i.e. -3, -1 and $+1°C$, respectively; Broecker, 1986). Similar Atlantic-Indian-Pacific contrasts were observed with the TF and MAT reconstructions (CLIMAP, 1981; Prell, 1985). Time averaging also smoothes the climate variability which renders difficult the comparison between deep-sea sediment and coral records. Indeed, Stott and Tang (1996) showed convincingly that for the tropical Atlantic about 10% of individual LGM planktonic foraminifera were influenced by extreme cooling (5–6°C), whereas most glacial specimens (80%) recorded temperatures that were within 2°C of the mean Holocene SST.

In addition, all paleoclimatic indicators mentioned above are imperfect paleothermometers because they are influenced by other factors than temperature (cf. Broecker, 1995 for a review of the problem) such as regional evaporation–precipitation balance and pH variations for the planktonic $\delta^{18}O$, humidity and CO_2 for pollen abundance and high altitude ice caps, gas supersaturation in groundwater aquifers, nutrient availability and thermocline structure for foraminiferal faunas and calcification rate for trace elements in corals. Some of these potential problems can be averaged out by replicating studies at numerous sites. The large number of variables affecting paleothermometers also justifies a multi-proxy approach which should ultimately lead to a proper evaluation of the respective biases and thus to concordant paleotemperatures for the glacial tropics.

For the present study we used the alkenone method (Brassell *et al.*, 1986; Prahl and Wakeham, 1987; Eglinton *et al.*, 1992) for evaluating temperature changes in the tropical Indian Ocean. Using a suite of deep-sea cores with high sedimentation rate (usually $> 10\,cm\,kyr^{-1}$) and detailed $\delta^{18}O$ planktonic stratigraphies, we reconstruct the surface temperatures which prevailed during the last glacial period. In addition, we studied in detail the last deglaciation in two cores: MD77194 raised at about 10°N, is characterized by a high sedimentation rate ($20\,cm\,kyr^{-1}$) supported by a detailed $\delta^{18}O$ curve, and MD79257 raised at about 20°S, is one of the best-dated deep-sea core of the Indian Ocean (more than twenty accelerator mass spectrometry AMS ^{14}C ages defining a mean sedimentation rate of about $50\,cm\,kyr^{-1}$, Duplessy *et al.*, 1991). These two cores allow us to study the timing of the deglacial warming in the tropical Indian Ocean.

SAMPLES AND METHODS

The 18 piston cores analysed for this study were sampled in the repositories of Museum National d'Histoire Naturelle de Paris (Indusom expeditions), Centre des Faibles Radioactivités in Gif-sur-Yvette (Osiris II, III, IV) and Netherland Oceanographic Research Center in Texel (NIOP2 expedition of the Dutch RV *Tyro*; van Weering *et al.*, 1997; Rostek *et al.*, 1997). In addition, two others cores from Indian Ocean were described previously (Rostek *et al.*, 1993; Emeis *et al.*, 1995a). These sediments were recovered from the tropical Indian Ocean between 20°S and 20°N of latitude and 40°E to 95°E of longitude (Fig. 1). A detailed $\delta^{18}O$ stratigraphy is available for each core usually measured on planktonic foraminiferas (see Fig. 2 and caption for details).

Gas chromatographic techniques used at CEREGE to quantify alkenones are described elsewhere (Sonzogni *et al.*, 1997). The analytical precision based on the multiple extraction, injection of the same duplicates of sediment samples, algal cultures and $C_{37:3Me}$ and $C_{37:2Me}$ synthetic alkenones is better than 0.3°C (i.e. 0.01 UK'_{37} units). Alkenone data are expressed in terms of unsaturation index of C37 alkenones (Prahl and Wakeham, 1987). All of our sediment samples are characterized by an absence of $C_{37:4Me}$, and a preponderance of $C_{37:2Me}$ over $C_{37:3Me}$ which is linked to the high SST prevailing in the tropical Indian Ocean. We thus used the simplified index $U^{K'}_{37}$ in this work since it is equal to the index U^{K}_{37} for temperatures warmer than 15°C (Prahl and Wakeham, 1987, Rosell-Melé *et al.*, 1994).

For each core, alkenones were measured in the top section (usually three samples or more) and the section

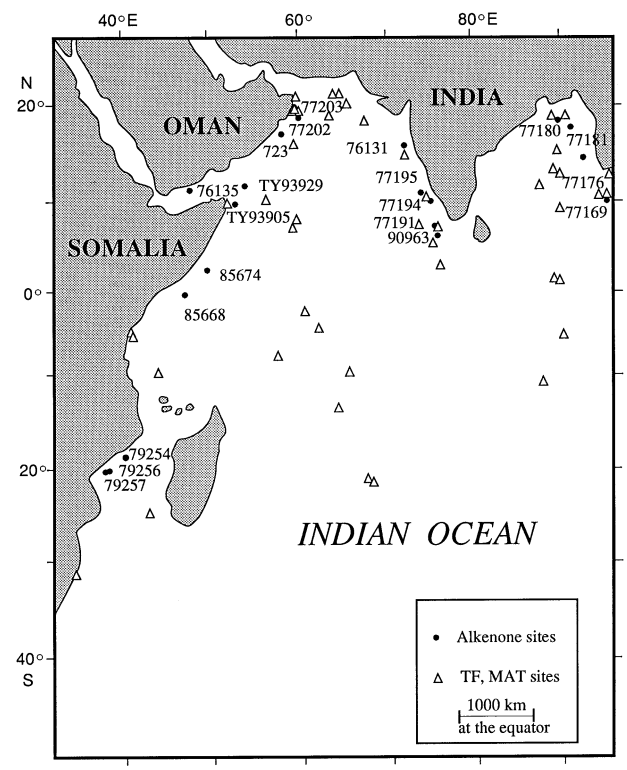

FIG. 1. Location of the deep-sea cores used to estimate the magnitude of glacial-interglacial temperature change by means of alkenones (20 closed dots, this work, and core MD90963 (Rostek *et al.*, 1993) and core ODP 723 (Emeis *et al.*, 1995a) and using transfer function (TF) and modern analog technique (MAT) (open triangles, Prell, 1985).

corresponding to the last glacial period identified using the $\delta^{18}O$ stratigraphy (usually three samples or more). Mean $U^{K'}_{37}$ value were calculated and compared for both periods (Table 1 and Fig. 3). Modern average $U^{K'}_{37}$ values vary between 0.897 in the Oman area and 1 in the Bay of Bengal (Fig. 3a). Glacial average $U^{K'}_{37}$ values ranges between 0.806 in the Oman area and 0.953 in the Bay of Bengal (Fig. 3b).

The $U^{K'}_{37}$ values can be converted into water temperatures using the standard equation established by Prahl *et al.* (1988) on cultures of *Emiliania huxleyi*: T (°C) = $(U^{K'}_{37} - 0.039)/0.034$. Studies of water column or sediment traps (Prahl and Wakeham, 1987) and recent sediments (Sikes *et al.*, 1991; Rosell-Melé *et al.*, 1995; Müller *et al.*, 1998) suggest that the calibration slope between 5 and 25°C is close to that by Prahl *et al.* (1988). Moreover, our separate study of 54 Indian Ocean core tops (including the tropical cores for which we have LGM sections) also indicates a general slope of 0.033 similar to that of the original calibration by Prahl *et al.* (Sonzogni *et al.*, 1997). Core-top calibrations are not as precise as true calibrations obtained by culturing algae, but they have the advantage to integrate (as do ancient sediments) the contributions of several strains, species or even genus of Prymnesiophytes. We thus feel that the calibration by Prahl *et al.* (1988) is appropriate as a first approximation. Nevertheless, for the high temperature range (> 24°C) it seems that the general calibration flattens out in a similar fashion as observed for the low-temperature range (Sikes and Volkman, 1993; Conte and Eglinton, 1993). By using 42 core tops from the Indian Ocean we have obtained the following relationship: T (°C) = $(U^{K'}_{37} - 0.317)/0.023$ which may be more applicable for reconstructing paleotemperatures for the tropical area (Sonzogni *et al.*, 1997). It is interesting to note that

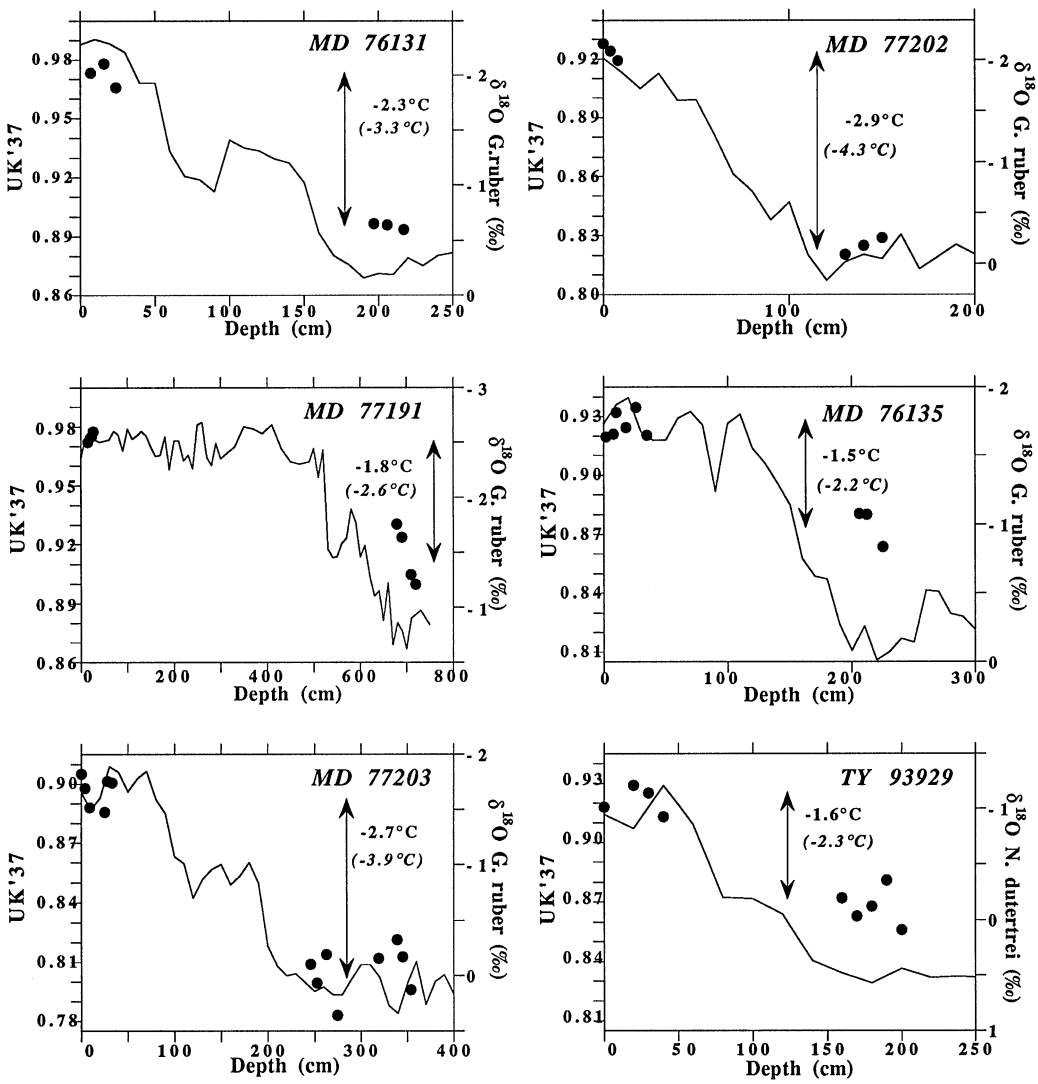

FIG. 2. Detailed stratigraphies for cores used in this work with published $\delta^{18}O$ records (Duplessy, 1982; Duplessy *et al.*, 1981,1991; Fontugne and Duplessy, 1986; Bassinot *et al.*, 1994; Vénec-Peyré *et al.*, 1995; Vergnaud-Grazzini *et al.*, 1995; Ganssen *et al.*, 1995). For each core, the LGM section has been identified according to the isotope stratigraphy (see also Kallel, 1988). Arrows indicate the magnitude of the glacial – interglacial temperature change (ΔSST) estimated using calibration equations by Prahl *et al.* (1988) and by Sonzogni *et al.* (1997) (in italic and parenthesis). In order to allow a visual comparison between cores, the different $U^{K'}_{37}$ axis have the same size in term of $U^{K'}_{37}$ units (0.14 ≈ 4°C, with the calibration of Prahl *et al.*, 1988). Note that for core MD77169 the LGM SST has been calculated by averaging measurements at 186 and 197 cm depth.

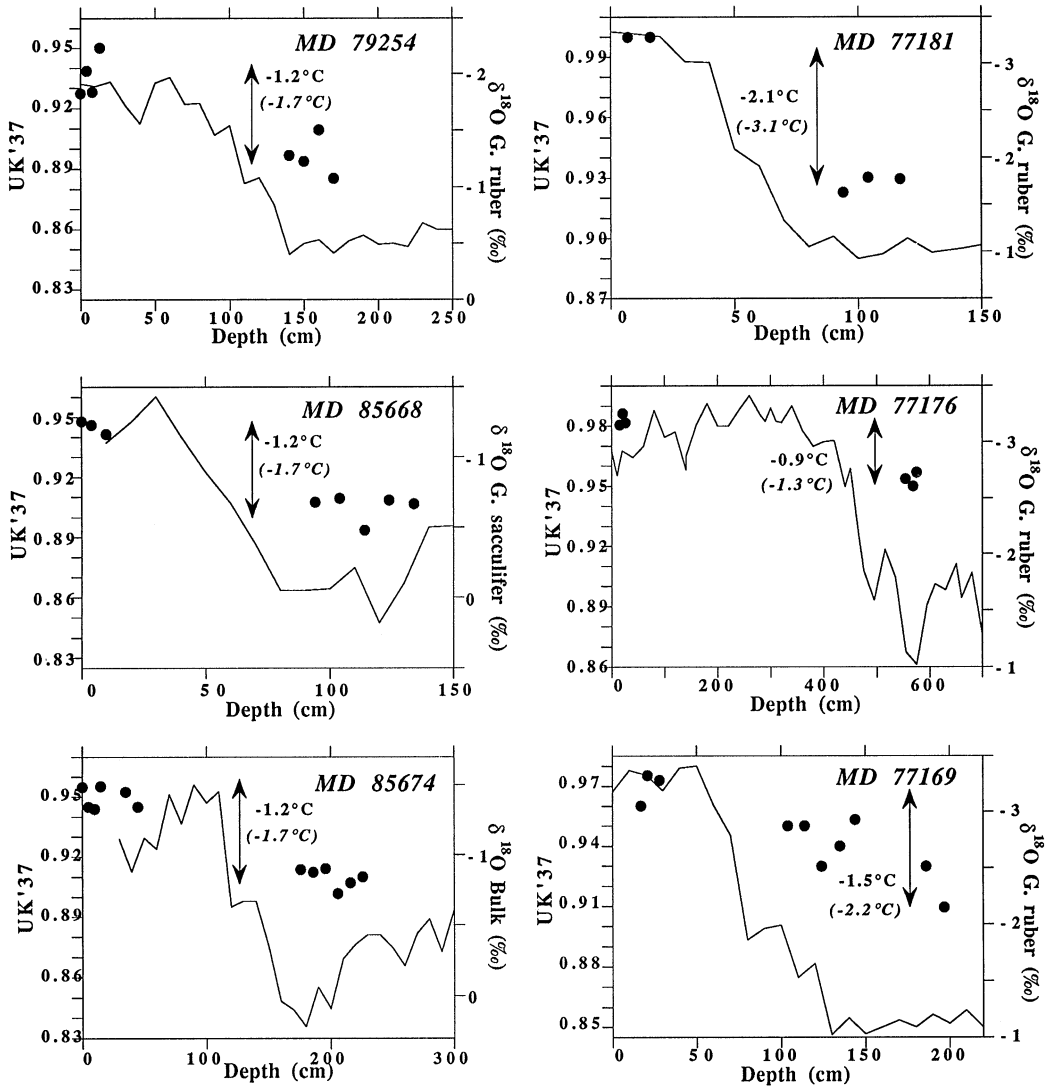

FIG. 2. (Continued)

a slope of 0.023 is also in the range observed by Prahl *et al.* (1995) for different strains of *E. huxleyi*. Furthermore, the reduction of the calibration slope for temperatures $> 24°C$ has been recently confirmed by culture studies performed on *E. huxleyi* and *Gephyrocapsa oceanica* (Conte *et al.*, 1998). As suggested by Volkman *et al.* (1995) and Conte *et al.* (1998), the true calibration may not be stricly linear but rather be sigmoidal in shape. Nevertheless, as a first approximation, the use of both linear slopes should bracket the actual magnitude of temperature changes.

Results and comparison with previous work

LGM-modern temperature contrast

The difference between modern and LGM temperatures (ΔSST) have been calculated and represented in Fig. 4a and b. By using the Prahl *et al.* (1988) equation, the average cooling is on the order of $-1.7°C$ with a standard deviation of 0.7°C (Table 1 and Fig. 4a). It is important to note that all ΔSST values are negative indicating colder temperatures during the glacial period (ranging from -0.2 to $-2.9°C$). These tropical records agree with previous alkenone profiles obtained from the Pacific (Lyle *et al.*, 1992; Ohkouchi *et al.*, 1994; Emeis *et al.*, 1995b) and the Atlantic (Eglinton *et al.*, 1992, Sikes and Keigwin, 1994, Schneider *et al.*, 1995).

In addition, we have compared the alkenone paleotemperatures with those of the CLIMAP reconstruction (1981) which has been further refined by Prell (1985) by comparing the TF and the MAT (Fig. 5). In order to be consistent with the alkenone study, the area of comparison has been restricted to the latitude range between 35°S and 25°N and the longitude range between 35°E to 95°E (locations of Prell's samples indicated in Fig. 1). ΔSST values estimated with alkenones, TF and MAT are compared in Fig. 5. In general, the ΔSST results based on alkenones are in broad agreement with the data derived from foraminifera (averages and standard deviations are: $-1.7 \pm 0.7°C$ with alkenones; $-0.8 \pm 1.3°C$ with $TF_{annual\ mean}$ and $0.1 \pm 0.7°C$ with $MAT_{annual\ mean}$).

TABLE 1. Unsaturation index ($U^{K'}_{37}$), sea-surface temperature (SST), Oxygen Isotope data for the 20 tropical Indian Ocean cores used in this work.

Core	UK′37 mean	ΔUK′37	SST (°C)	ΔSST	SST* (°C)	ΔSST*	∂180(‰) mean	Δ∂180	∂180 ref
MD79254									
Modern	0.936	0.04	26.4	− 1.2	26.8	− 1.7	− 1.91	− 1.45	Van Campo
LGM	0.896		25.2		25.1		− 0.46		*et al.* (1990)
MD79257									
Modern	0.959	0.07	27.1	− 2.2	27.8	− 3.2	− 1.83	− 1.28	Duplessy
LGM	0.884		24.9		24.5		− 0.55		*et al.* (1991)
MD79256									
Modern	0.937	0.04	26.4	− 1.0	26.8	− 1.5			
LGM	0.901		25.4		25.3				
MD85668									
Modern	0.945	0.04	26.7	− 1.2	27.2	− 1.7	− 1.18	− 1.00	Vénec-Peyré
LGM	0.905		25.5		25.4		− 0.18		*et al.* (1995)
MD85674									
Modern	0.949	0.04	26.8	− 1.2	27.4	− 1.7	− 0.99	− 0.92	Vergnaud-
LGM	0.910		25.6		25.6		− 0.07		Grazzini *et al.* (1995)
MD77180									
Modern	0.982	0.05	27.7	− 1.5	28.8	− 2.1	− 3.39	− 2.52	Duplessy
LGM	0.932		26.3		26.6		− 0.87		(1982)
MD77181									
Modern	1.000	0.07	28.3	− 2.1	29.5	− 3.1	− 3.31	− 2.27	Duplessy
LGM	0.927		26.1		26.4		− 1.04		(1982)
MD77176									
Modern	0.983	0.03	27.8	− 0.9	28.8	− 1.3	− 2.84	− 1.47	Duplessy
LGM	0.953		26.9		27.5		− 1.37		(1982)
MD77169									
Modern	0.969	0.05	27.4	− 1.5	28.2	− 2.2	− 3.26	− 2.13	Fontugne and
LGM	0.920		25.9		26.1		− 1.13		Duplessy (1986)
MD76131									
Modern	0.972	0.08	27.5	− 2.3	28.3	− 3.3	− 2.30	− 2.08	Duplessy
LGM	0.895		25.2		25.0		− 0.22		*et al.* (1981)
MD77195									
Modern	0.967	0.05	27.3	− 1.5	28.1	− 2.2	− 2.44	− 1.98	Duplessy
LGM	0.917		25.8		26.0		− 0.46		(1982)
MD77194									
Modern	0.972	0.06	27.4	− 1.8	28.3	− 2.6	− 2.47	− 1.76	Duplessy
LGM	0.913		25.7		25.8		− 0.71		*et al.* (1981)
MD77191									
Modern	0.975	0.06	27.5	− 1.8	28.5	− 2.6	− 2.53	− 1.74	Duplessy
LGM	0.915		25.8		25.9		− 0.79		(1982)
MD77203									
Modern	0.897	0.09	25.2	− 2.7	25.1	− 3.9	− 1.69	− 1.81	Fontugne and
LGM	0.806		22.6		21.2		0.12		Duplessy (1986)
MD77202									
Modern	0.924	0.10	26.0	− 2.9	26.2	− 4.3	− 1.95	− 1.90	Duplessy
LGM	0.825		23.1		22.0		− 0.05		*et al.* (1981)
MD76135									
Modern	0.925	0.05	26.1	− 1.5	26.3	− 2.2	− 1.79	− 1.68	Duplessy
LGM	0.875		24.6		24.1		− 0.11		(1982)
MD90963									
Modern	0.991	0.08	28.0	− 2.5	29.2	− 3.6	− 2.58	− 1.61	Bassinot
LGM	0.907		25.5		25.5		− 0.97		*et al.* (1994)
TY93929/P									
Modern	0.921	0.05	26.0	− 1.6	26.1	− 2.3	− 0.99	− 1.50	Ganssen
LGM	0.868		24.4		23.8		0.51		*et al.*, 1995
TY93905/P									
Modern	0.929	0.01	26.2	− 0.2	26.5	− 0.3			
LGM	0.922		26.0		26.2				
ODP Site 723									
Modern	0.903	0.07	25.4	− 2.0	25.3	− 2.9	− 0.90	–1.65	Emeis *et al.*
LGM	0.835		23.4		22.4		0.75		(1995a)

Note: $U^{K'}_{37}$: unsaturation index for C37 alkenone, i.e. $[C_{37:2Me}]/[C_{37:3Me}] + [C_{37:2Me}]$ (Prahl and Wakeham, 1987); SST: sea surface temperature estimated using the equation: SST (°C) = $(U^{K'}_{37} - 0.039)/0.034$ of Prahl *et al.* (1988); SST*: sea surface temperature estimated using the equation SST (°C) = $(U^{K'}_{37} - 0.317)/0.0{\cdot}23$ of Sonzogni *et al.* (1997); ΔSST = magnitude of the glacial-modern contrast of temperature; Δ∂18O = magniture of the glacial-modern contrast of $\delta^{18}O$.

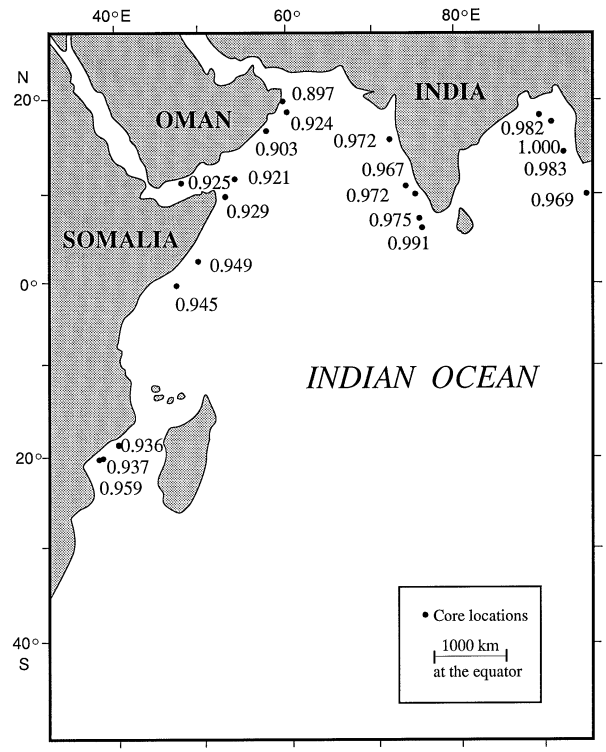

(a)

FIG. 3. (a) Mean modern unsaturation index ($U^{K'}_{37}$) values for the 20 core tops.

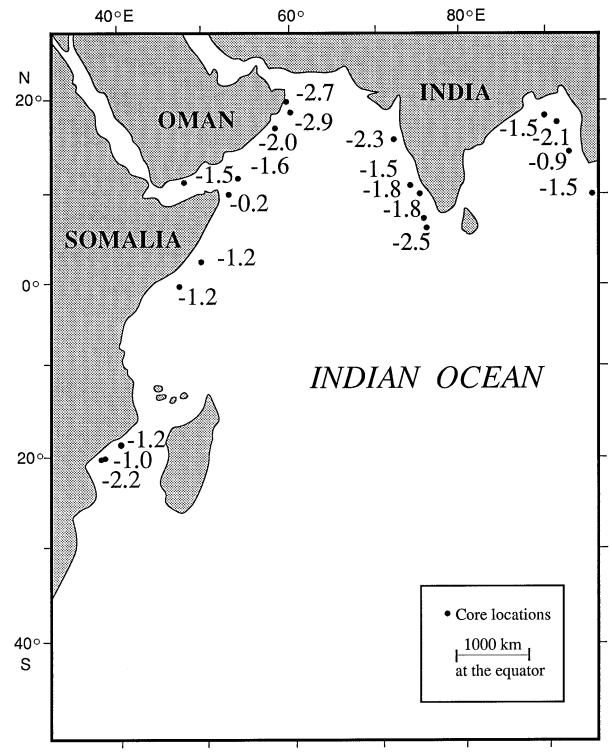

(a)

FIG. 4. (a) Magnitude of the glacial-modern temperature contrast (ΔSST) for 20 Indian Ocean deep-sea cores. The unsaturation index ($U^{K'}_{37}$) has been converted in term of temperature by using the calibration of Prahl *et al.* (1988).

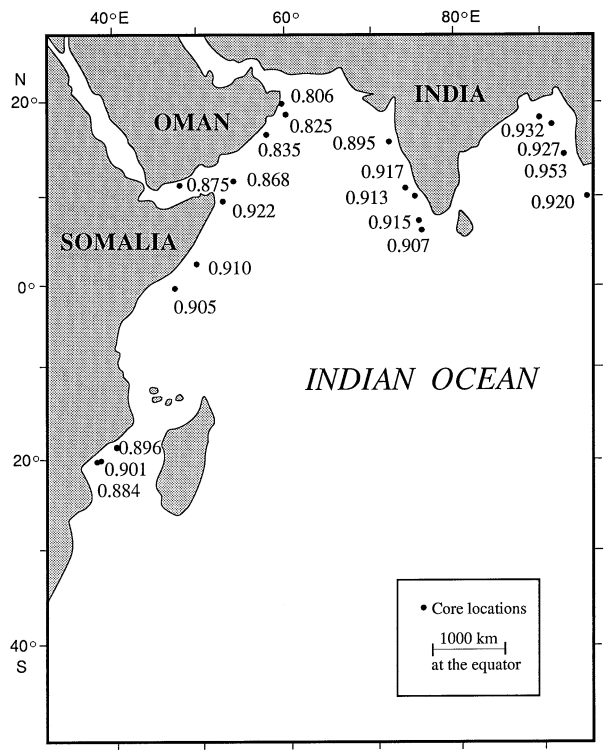

(b)

FIG. 3. (b) Mean glacial unsaturation index ($U^{K'}_{37}$) values for the 20 cores.

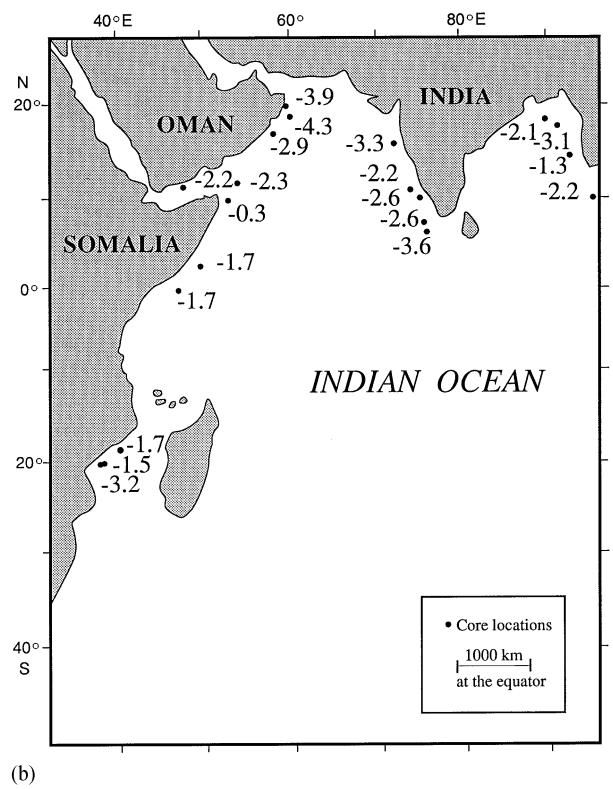

(b)

FIG. 4. (b) Magnitude of the glacial-modern temperature contrast (ΔSST) for 20 Indian Ocean deep-sea cores. The unsaturation index ($U^{K'}_{37}$) has been converted in term of temperature by using the calibration of Sonzogni *et al.* (1997) for temperature $> 24°C$.

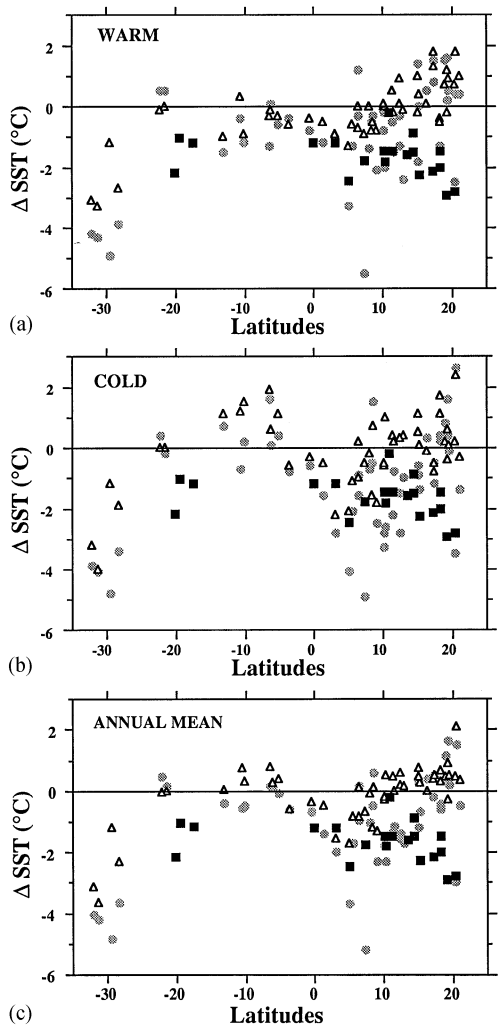

FIG. 5a–c. Magnitude of the glacial-modern temperature contrast (ΔSST) in the Indian Ocean between 35°S and 25°N. Black squares are for alkenone estimates (this work, calculated with the calibration of Prahl *et al.*, 1988), grey circles for transfer function estimates (TF, Prell, 1985) and open triangles for modern analog technique estimates (MAT, Prell, 1985) for the warm season (a), the cold season (b) and the annual mean (c). The ΔSST averages and standard deviations are -1.7 ± 0.7°C with alkenones; -0.6 ± 1.4°C with TF_{warm}; -0.9 ± 1.6°C with TF_{cold} and $+0.0 \pm 0.7$°C with MAT_{warm}, $+0.1 \pm 1.0$°C with MAT_{cold}. Note that for the sake of the comparison with our alkenone data, we have only used foraminifera data obtained in the longitude range 40°E–95°E and the latitudinal range 23°S–23°N for the Indian Ocean. For the latitude between 10° and 22°N it comes -1.7 ± 0.7°C with alkenones, -0.3 ± 1.3°C with TF_{warm}, -0.9 ± 1.6°C with TF_{cold} and $+0.5 \pm 0.7$°C with MAT_{warm}, $+0.3 \pm 0.7$°C with MAT_{cold}.

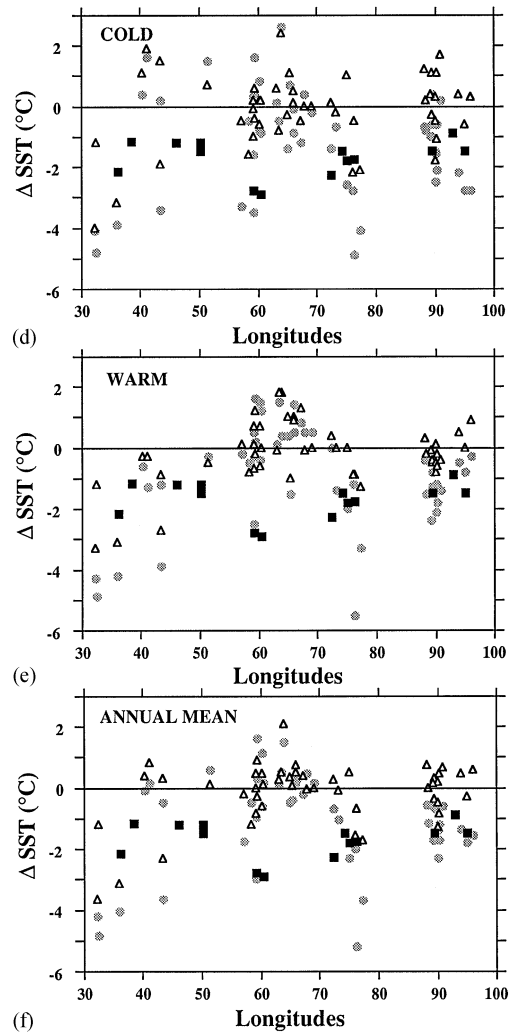

FIG. 5d–f. Magnitude of the glacial-modern temperature contrast (ΔSST) in the Indian Ocean between 30°E and 100°E. Black squares are for alkenone estimates (this work, calculated with the calibration of Prahl *et al.*, 1988), grey circles for transfer function estimates (TF, Prell, 1985) and open triangles for modern analog technique estimates (MAT, Prell, 1985) for the warm season (d), the cold season (e) and the annual mean (f).

Nevertheless, alkenones indicate that glacial temperatures were systematically colder than today (negative ΔSST ranging between -0.2 and -2.9°C), whereas CLIMAP data show several positives anomalies with LGM warmer than today ($TF_{annual\ mean}$ ΔSST ranging between -5.2 and $+1.6$°C and $MAT_{annual\ mean}$ ΔSST ranging between -1.7 and $+2.1$°C). As can be seen clearly in Fig. 5a–c the maximum difference between the two data sets is located between 10° and 22°N for which MAT predict little change (Mean ΔSST = $+0.4$ and S.D. = 0.5°C with $MAT_{annual\ mean}$), whereas alkenones predict a colder LGM than today (Mean ΔSST = -1.7 and S.D. = 0.7°C). This difference between estimates based on foraminifera and alkenone between 10°N and 22°N is not due to a systematic difference in the location of the cores. In this latitude range, we measured alkenones in six of the same cores used by Prell (1985) in his TF-MAT comparison (included in Fig. 5). For the four cores from the Arabian Sea, the average ΔSST are: -2.2°C with alkenones and -0.1°C with $MAT_{annual\ mean}$. For the two cores from the Bay of Bengal, the average ΔSST are: -1.5°C with alkenones and 0.0°C with $MAT_{annual\ mean}$. It thus appears that the LGM estimates with MAT are slightly but systematically warmer than with alkenones in cores between 10°N and 22°N. This confirms the overall impression based in Fig. 5 which is thus not an artifact of core location.

TABLE 2. Compilation of the magnitude of glacial-modern temperature contrast (ΔSST) estimated using alkenones, transfer function (TF) and modern analog technique (MAT) in tropical Indian, Pacific and Atlantic deep-sea cores. ΔSST based on Sr and U in corals from Barbados have also been added. ± corresponds to the standard deviation of the core population. For the sake of the comparison with our alkenone data, we have only used foraminifera data obtained in the longitude range 40–95°E and the latitudinal range 23°S–23°N for the Indian Ocean.

SST estimate method	Core ID	Latitude	Longitude	ΔSST (°C) LGM-Mod	Reference
Indidan Ocean					
Alkenones	*MD*79254	17°53 S	38°40 E	− 1.2	This paper
Alkenones	MD79257	20°24 S	36°20 E	− 2.2	This paper
Alkenones	MD79256	19°35 S	37°02 E	− 1.0	This paper
Alkenones	MD85668	0°01 S	46°02 E	− 1.2	This paper
Alkenones	MD85674	3°11 N	50°26 E	− 1.2	This paper
Alkenones	MD77180	18°28 N	89°51 E	− 1.5	This paper
Alkenones	MD77181	17°24 N	90°29 E	− 2.1	This paper
Alkenones	MD77176	14°31 N	93°08 E	− 0.9	This paper
Alkenones	MD77169	10°13 N	95°03 E	− 1.5	This paper
Alkenones	MD76131	15°32 N	72°34 E	− 2.3	This paper
Alkenones	MD77195	11°30 N	74°32 E	− 1.5	This paper
Alkenones	MD77194	10°28 N	75°14 E	− 1.8	This paper
Alkenones	MD77191	7°30 N	76°43 E	− 1.8	This paper
Alkenones	MD77203	20°42 N	59°34 E	− 2.7	This paper
Alkenones	MD77202	19°13 N	60°41 E	− 2.9	This paper
Alkenones	MD76135	14°27 N	50°31 E	− 1.5	This paper
Alkenones	MD90963	5°04 N	73°53 E	− 2.5	Rostek *et al.* (1993)
Alkenones	TY93929/P	13°42 N	53°15 E	− 1.6	This paper
Alkenones	TY93905/P	10°54 N	51°56 E	− 0.2	This paper
Alkenones	ODP Site 723	18°04 N	57°36 E	− 2.0	Emeis *et al.* (1995a)
			Average alk	− 1.7 ± 0.7	
Foram. assemblages					
TF cold	44 cores	23°S–23°N	40°E–95°E	− 0.9 ± 1.6	CLIMAP (1981); Prell (1985)
TF warm	44 cores	23°S–23°N	40°E–95°E	− 0.6 ± 1.4	CLIMAP (1981); Prell (1985)
MAT cold	44 cores	23°S–23°N	40°E–95°E	+ 0.1 ± 1.0	Prell (1985)
MAT warm	44 cores	23°S–23°N	40°E–95°E	+ 0.0 ± 0.7	Prell (1985)
TF	RC 27–23	18°00 N	57°60 E	0.0	Anderson and Thunnel (1993)
MAT	RC 27–23	18°00 N	57°60 E	+ 3.0	Anderson and Thunnel (1993)
Pacific Ocean					
Alkenones	KH92-1-5cBX	3°32N	141°5E	− 0.5	Ohkouchi *et al.* (1994)
Alkenones	ODP Site846	3°05S	90°49W	− 1.2	Emeis *et al.* (1995b)
Alkenones	W8402A-14Gc	0°57N	138°57W	− 1.3	Prahl *et al.* (1989) Lyle *et al.* (1992)
			Average alk	− 1.0 ± 0.4	
Foram. assemblages					
TF cold	26 cores	20°S–20°N	80°E–120°E	− 1.4 ± 4.0	CLIMAP (1981); Prell (1985)
TF warm	26 cores	20°S–20°N	80°E–120°E	+ 1.2 ± 1.6	CLIMAP (1981); Prell (1985)
MAT cold	26 cores	20°S–20°N	80°E–120°E	− 0.2 ± 2.5	Prell (1985)
MAT warm	26 cores	20°S–20°N	80°E–120°E	+ 0.6 ± 1.1	Prell (1985)
MAT	12 cores	20°S–20°N	80°W–120°E	− 0.6 ± 0.9	Anderson *et al.* (1989) Miao *et al.* (1994) Thunnel *et al.* (1994)
Atlantic Ocean					
Alkenones	BOFS31K	1 9°00N	20°10W	− 3.0	Zhao *et al.* (1995)
Alkenones	Site 658	20°45N	18°35W	− 4.3	Eglinton *et al.* (1992); Zhao *et al.* (1993)
Alkenones	Geob1105–4	1°39S	12°2E	− 3.2	Schneider *et al.* (1995)
Alkenones	Geob1008–3	6°3S	10°2E	− 4.4	Schneider *et al.* (1995)
Alkenones	Geob1016–3	11°5S	11°4E	− 3.6	Schneider *et al.* (1995)
Alkenones	Geob1028–5	20°06S	9°11E	− 4.1	Schneider *et al.* (1995)
Alkenones	12PC51	0°00N	22°59W	− 2.4	Sikes and Keigwin (1994)
Alkenones	M16415–2	9°N	19°W	− 3.5	Brassell *et al.* (1986)
			Average alk	− 3.6 ± 0.7	
Foram. assemblages					
TF cold	78 cores	20°S–20°N	80°W–20°E	− 3.1 ± 1.8	CLIMAP (1981); Prell (1985)
TF warm	78 cores	20°S–20°N	80°W–20°E	− 1.2 ± 1.9	CLIMAP (1981); Prell (1985)
MAT cold	78 cores	20°S–20°N	80°W–20°E	− 2.4 ± 2.0	Prell (1985)
MAT warm	78 cores	20°S–20°N	80°W–20°E	− 1.1 ± 1.6	Prell (1985)
Strontium	corals	13°02 N	59°34W	− 5–6°C	Guilderson *et al.* (1994)
Uranium	corals	13°02 N	59°34W	− 5–6°C	Min *et al.* (1995)

In addition, the $\Delta SST_{alkenones}$ have been compared to the ΔSST_{TF} and ΔSST_{MAT} and plotted versus longitudes (Fig. 5d–f). The main difference between alkenones and the ΔSST_{TF} and ΔSST_{MAT} is located in the western Arabian Sea (55–65°E). Indeed, in this area, foraminifera data show clearly a positive ΔSST while alkenone estimates indicate a negative ΔSST. Although more alkenone data are needed, there is no clear relation with boundary currents and upwelling zones.

Similarly, we observe no simple relationship between the percentage of *Globigerina bulloides*, an upwelling indicator, and ΔSST on the six cores in which both time series are available. Indeed, the LGM percentage of *G. bulloides* is higher than modern for cores MD76131, MD77195 but lower for cores MD76135, MD77169, MD77176, MD77191 (Cayre, 1997). In any case, work in progress at CEREGE show that a better approach is to take into account the entire foraminifera distribution in order to derive a transfer function to quantify the paleoproductivity (Cayre *et al.*, 1998).

As previously discussed there are still differences of opinion concerning the calibration to be applied to convert accurately the measured $U^{K'}_{37}$ shifts in terms of temperature. Since the Indian Ocean core tops seem to indicate a reduction of the calibration slope above 24°C (Sonzogni *et al.*, 1997), we have tentatively calculated a second estimate of ΔSST for each deep sea core (Table 1 and Fig. 4b). As expected the second calibration predicts that the LGM period was even colder than previously derived with the standard calibration based on *E. huxleyi* culture (Prahl *et al.*, 1988), but none of the individual ΔSST is larger than -4°C in magnitude. According to the difference in calibration slopes, the ΔSST calculated with the local calibration are 40% larger than by using the culture relationship by Prahl *et al.* (1988). This 40% difference remains modest in the context of the comparison with estimates based on foraminifera, corals, pollens and noble gas concentrations. The average cooling is -2.4°C vs -1.7°C (for the first one) with a standard deviation of -0.7°C on the 20 cores population. It is thus clear that the temperature changes estimated with alkenones are smaller than the dramatic 5–6°C cooling inferred from trace elements measured in tropical corals (Beck *et al.*, 1992; Guilderson *et al.*, 1994; Min *et al.*, 1995).

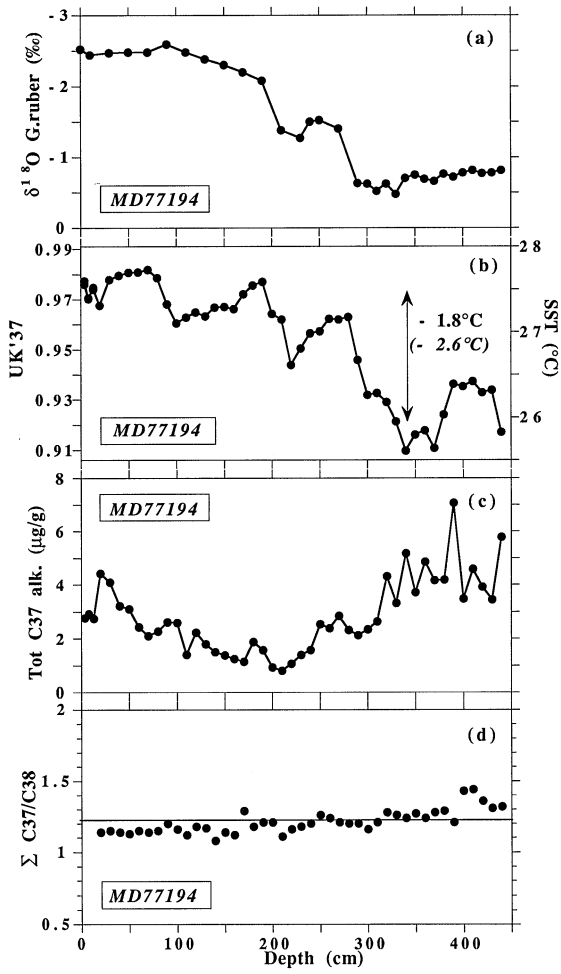

FIG. 6. Paleoclimatic records for Core MD77194 (10°28′N, 75°14′E, depth: 1222 m) (a) $\delta^{18}O$ stratigraphy measured on the planktonic foraminifera *Globigerinoides ruber* (Duplessy *et al.*, 1981). (b) Depth record of $U^{K'}_{37}$. The SST axis is constructed with the calibration by Prahl *et al.* (1988). The arrow indicates the magnitude of the glacial-modern temperature contrast estimated using calibrations by Prahl *et al.* (1988) and Sonzogni *et al.* (1997) (italic and parenthesis). (c) Depth record of the total C37 alkenone concentration (µg g^{-1} of dry sediment). (d) Depth record of the ratios total C37 alkenone/total C38 alkenone (ΣC37/C38) (mean = 1.21, range = 1.08–1.44, S.D. = 0.08, $n = 46$).

The last deglaciation at 10°N

Core MD77194 was collected off the southwest coast of India in the eastern part of the Arabian Sea (10°28′N, 75°14′E; water depth of 1222 m). This core has a clear stratigraphy based on $\delta^{18}O$ measured on the planktonic foraminifera *Globigerinoides ruber* (Fig. 6a; Duplessy *et al.*, 1981). In order to place the stratigraphic record on an absolute time scale, we correlated the $\delta^{18}O$ record of MD77194 with that of core 74KL from the western Arabian Sea which is dated by ^{14}C (Sirocko *et al.*, 1993). Several tie points have been identified at 200 cm (≈11.8 cal kyr BP), 233 cm (≈13.3 cal kyr BP), 282 cm (≈14.9 cal kyr BP) and 303 cm (≈16.3 cal kyr BP) (Fig. 7). By using this first-order chronology, it is possible to conclude that the sedimentation rate was about 25 cm kyr^{-1} during the last deglaciation and 17 cm kyr^{-1} during the Holocene period. The sampling interval for alkenone measurements is 10 cm which corresponds to a time interval smaller than 0.5 kyr (Table 3).

As can be seen clearly in Fig. 6a and b, the last deglaciation exhibits a two-step character for both $\delta^{18}O$ and SST records. Coldest temperatures of about 25.5–26°C occurred during the LGM and are followed by a significant 1.5°C warming culminating at about 14.9 cal kyr BP, in phase with the Bölling initial warming dated in Greenland (Alley *et al.*, 1993; Hammer

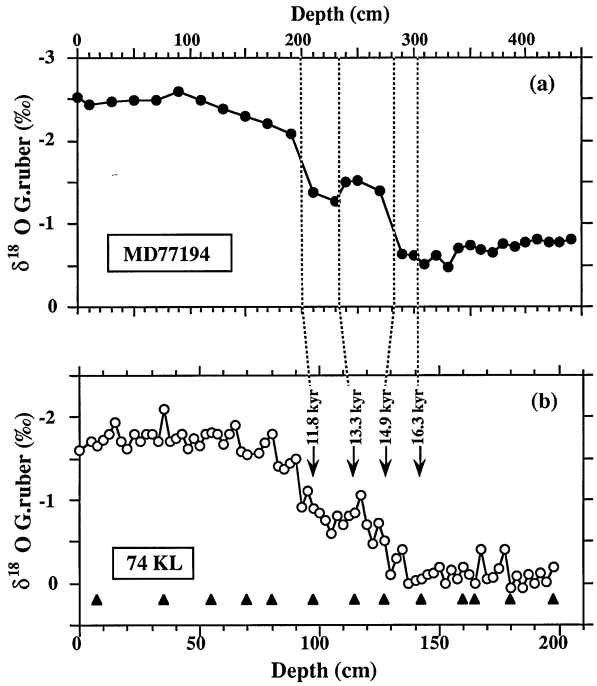

FIG. 7. Correlation between the $\delta^{18}O$ records obtained for core MD77194 (10°28′N, 75°14′E) and 74 KL (14°19N, 57°20E) from the Arabian Sea. Core 74 KL is dated by AMS-^{14}C (Sirocko *et al.*, 1993). ^{14}C ages are corrected for reservoir age (800 yr, Uerpmann, 1991) and calibrated into calendar ages by using U–Th ages in corals (Bard *et al.*, 1990, 1993). Several tie points have been identified for core MD77194: 200 cm ≈ 11,800 cal yr BP, 233 cm ≈ 13,300 cal yr BP, 282 cm ≈ 14,900 cal yr BP and at 303 cm ≈ 16,300 cal yr BP (triangles indicate the 13 age control points based on ^{14}C ages).

et al., 1997). Alkenones record a small temperature decrease between 13.3 and 12.3 cal kyr BP cm concomitant with a clear $\delta^{18}O$ maximum. The second step of the last deglaciation is centered at about 210 cm and characterized by a sharp 1°C increase of the temperatures and a marked $\delta^{18}O$ decrease. The Holocene section exhibits a rather stable and high temperature ranging between 27.1 and 27.7°C which is close to the modern annual mean of 28.4°C according to the World Ocean Atlas (Levitus, 1994). On average, the LGM was thus about 1.8°C colder than today or 2.6°C colder using the smaller calibration slope derived from Indian Ocean core tops (Sonzogni *et al.*, 1997).

The paleotemperature record obtained for core MD77194 can be compared with that reconstructed for core RC27-23 from the western Arabian Sea (Anderson and Thunell, 1993). Although both $\delta^{18}O$ curves are similar in shape and timing, the temperature time series are different: the MAT indicates no change at all while the TF technique leads to a gradual *cooling* of about 3°C during the last deglaciation. The alkenone time series is probably closer to the truth because the $\delta^{18}O$ and $U^{K'}_{37}$ records are fluctuating in phase which is even the case for the transient event centered at about 12 cal kyr BP. The discrepancy observed between results derived by the MAT and TF techniques also suggests that there is something amiss in the inherent assumption that the present day foraminifera distribution can be used as a modern analog for past faunal distribution in this particular area. As discussed by Anderson and Thunnel (1993) this conclusion has several important implications for interpreting the $\delta^{18}O$ signal.

In addition, the total abundance of alkenones has been quantified in order to evaluate qualitatively the

TABLE 3. Alkenone data for core MD77194 (10°28′N, 75°14′E, depth: 1222 m)

Depth (cm)	C37 total μg g^{-1}	Σ37/38	$U^{K'}_{37}$	SST (°C)
4	2.77		0.976	27.6
8	2.92		0.970	27.4
13	2.75		0.975	27.5
20	4.42	1.19	0.968	27.3
30	4.09	1.15	0.978	27.6
40	3.21	1.14	0.979	27.7
50	3.10	1.13	0.981	27.7
60	2.43	1.15	0.981	27.7
70	2.11	1.14	0.982	27.7
80	2.28	1.15	0.979	27.6
90	2.61	1.20	0.968	27.3
100	2.59	1.16	0.961	27.1
110	1.40	1.12	0.963	27.2
120	2.23	1.18	0.965	27.2
130	1.80	1.17	0.963	27.2
140	1.50	1.08	0.967	27.3
150	1.38	1.14	0.967	27.3
160	1.25	1.12	0.966	27.3
170	1.14	1.29	0.972	27.4
180	1.88	1.18	0.976	27.5
190	1.58	1.21	0.977	27.6
200	0.93	1.21	0.964	27.2
210	0.80	1.11	0.962	27.1
220	1.07	1.16	0.944	26.6
230	1.39	1.18	0.950	26.8
240	1.58	1.20	0.956	27.0
250	2.54	1.26	0.957	27.0
260	2.39	1.24	0.962	27.2
270	2.84	1.21	0.962	27.1
280	2.32	1.20	0.963	27.2
290	2.13	1.20	0.946	26.7
300	2.34	1.16	0.932	26.3
310	2.64	1.21	0.933	26.3
320	4.31	1.28	0.929	26.2
330	3.32	1.26	0.921	25.9
340	5.18	1.24	0.910	25.6
350	3.71	1.27	0.916	25.8
360	4.85	1.24	0.918	25.8
370	4.16	1.28	0.911	25.6
380	4.19	1.21	0.924	26.0
390	7.07	1.43	0.936	26.4
400	3.47	1.44	0.935	26.4
410	4.58	1.36	0.937	26.4
420	3.92	1.31	0.933	26.3
430	3.44	1.32	0.934	26.3
440	5.78	1.33	0.917	25.8

Note: C37 Total: C_{37} alkenone concentration (C37:3Me + C37:2Me) in μg per g of dry sediment; Σ37/38: (Total C37 alkenone)/(total C38 alkenone); $U^{K'}_{37}$: unsaturation index for C37 alkenone, i.e. $[C_{37:2Me}]/([C_{37:3Me}] + [C_{37:2Me}])$; SST: sea surface temperature estimated using the equation: SST (°C) = $(U^{K'}_{37} - 0.039)/0.034$ of Prahl *et al.* (1988).

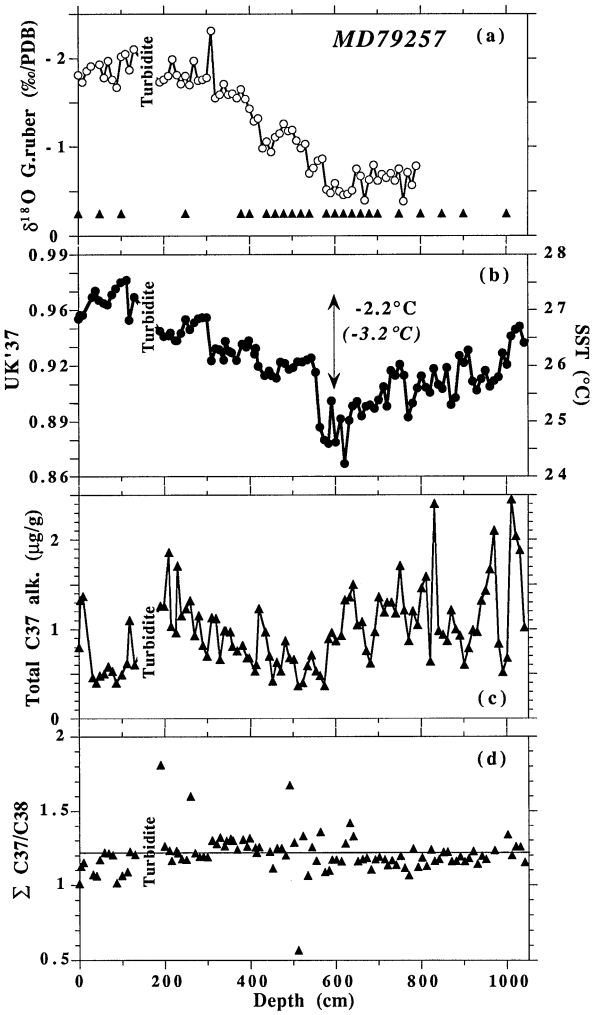

FIG. 8. Paleoclimatic records for Core MD 79257 (20°24′S, 36°20′E, depth: 1262 m): (a) $\delta^{18}O$ stratigraphy measured on the planktonic foraminifera *G. ruber* (Duplesssy et al., 1991; Caralp *et al.*, 1993). Triangles indicate the age control points which are based on AMS-^{14}C dating of *G. ruber* (Duplessy *et al.*, 1991). (b) Depth record of $U^{K'}_{37}$. The SST axis is constructed with the calibration by Prahl *et al.* (1988). The arrow indicates the magnitude of the glacial-modern temperature contrast estimated using calibrations by Prahl *et al.* (1988) and Sonzogni *et al.* (1997) (italic and parenthesis). (c) Depth record of the total C_{37} alkenone concentration ($\mu g\, g^{-1}$ of dry sediment). (d) Depth record of the ratios total C37 alkenone/total C38 alkenone (ΣC37/C38) (mean = 1.21, range = 0.57–1.81, S.D. = 0.13, $n = 102$).

paleoproductivity in the eastern Arabian Sea (Fig. 6c). The total C37 alkenones is relatively high and fluctuates between about 1 $\mu g\, g^{-1}$ at 210 cm and more than 7 $\mu g\, g^{-1}$ at 390 cm. The alkenones concentration is thus significantly higher in the glacial (weighted mean $\approx 4\ \mu g\, g^{-1}$) than in the Holocene section of the core (weighted mean $\approx 2\ \mu g\, g^{-1}$). Mass accumulation rates of alkenones should be calculated in order to better assess the changes of productivity. However, even in the absence of direct ^{14}C measurement, it is possible to conclude that the alkenone mass accumulation rate was higher during the Late Glacial than during the Holocene because the sedimentation rate is higher (≈ 25 cm kyr^{-1}) during the period between 16.3 and 11.8 cal kyr BP than after 11.8 cal kyr BP (≈ 17 cm kyr^{-1}). An increased productivity during the glacial periods was already derived from other Arabian Sea cores by analyzing total organic carbon and alkenone mass accumulation rate (Rostek *et al.*, 1994, 1997) and by considering productivity proxies based on coccoliths and foraminifera distributions (Beaufort *et al.*, 1997; Cayre *et al.*, 1998, Rostek *et al.*, 1997). For the low latitudes of the other oceans, a widespread productivity increase has been previously reported during the glacial periods (Müller *et al.*, 1983; Herguera and Berger, 1994).

In the Indian Ocean, an increased productivity during the glacial period would be in apparent conflict with a weakening of the summer SW-monsoon hypothesized previously (Prell and Kutzbach, 1987; Clemens *et al.*, 1991; Anderson and Prell, 1993). This discrepancy may be reconciled if the increased productivity was a consequence of a strengthening of the winter NE monsoon leading to a deepening of the mixed layer (Rostek *et al.*, 1994, 1997).

The last deglaciation at 20°S

Core MD79257 was collected in the southern part of the Mozambique Channel (20°24′S, 36°20′E, water depth 1262 m) and details on the lithology can be found in the work by Caralp *et al.* (1993). $\delta^{18}O$ ratios have been measured on planktonic and benthic foraminifera and numerous ^{14}C ages were obtained by AMS (Duplessy *et al.*, 1991). The sampling interval for alkenone measurements is 10 cm and thus corresponds to an average resolution of about 0.2 kyr (Table 4).

We have converted the ^{14}C ages into calendar ages by using the ^{14}C calibration based on U–Th dating of corals (Bard *et al.*, 1990, 1993). By using polynomial fits we then constructed a continuous calendar chronology for the entire MD79257 core (Fig. 9). Throughout the last 45 kyr, the sedimentation rate was high (≈ 50 cm kyr^{-1}) with a minimum during the last 7 cal kyr BP (22 cm kyr^{-1}) and a prominent maximum centered at about 8 cal kyr BP (up to 260 cm kyr^{-1}). The period between 10 and 45 cal kyr BP is characterized by a sedimentation rate of intermediate magnitude (25 cm kyr^{-1}). The high sedimentation rate observed around 8 cal kyr BP has been attributed to a dramatic increase of the detrital input from the Zambezi River linked to a rainfall maximum over the african continent (Vincens, 1989; Caralp *et al.*, 1993).

To a first order, SST and $\delta^{18}O$ variations are in phase with warmer temperatures during the Holocene and colder temperatures during the Last Glacial period (Fig. 10). An abrupt 1.5°C warming at 15.1 cal kyr BP is followed by a transitory pause until 12.4 cal kyr BP. The second part of the last deglaciation is more complex and less abrupt than the first one: a 1°C warming took place between ≈ 11 and 7 cal kyr BP. The core top temperature is 26.9°C which is close to the modern annual mean of 25.8°C calculated with the World Ocean Atlas (Levitus, 1994). The magnitude of

the deglacial warming is thus of the order of 2.5°C which is at the high end of our set of 20 cores. The contrast is larger by 1°C (i.e. ≈3.5°C colder) by using the smaller calibration slope derived from Indian Ocean core tops for temperatures > 24°C (Sonzogni *et al*., 1997).

It is interesting to note that the transient between 12.2 and ≈11.5 cal kyr BP suggested by the $U^{K'}_{37}$ record is also clearly represented in the $\delta^{18}O$ profile measured for *G. ruber*. Furthermore, there is a clear synchroneity between these two independent transitory features and the Younger Dryas cold period observed in North-Atlantic and European climate records (e.g. Bard *et al*., 1987; Johnsen *et al*., 1992; Alley *et al*., 1993; Goslar *et al*., 1995). However, the reversal in core MD79257 does not correspond to a return to full glacial conditions as is the case for Greenland records (cf. Fig. 10c).

The reversal in core MD79257 is similar in relative amplitude to the one observed in climate records from Antarctica but the warming steps are distinctly younger (Hammer *et al*., 1994; Sowers and Bender, 1995; Jouzel *et al*., 1995; see Fig. 10d). Antarctica temperatures began to rise between 18 and 20 cal kyr BP, i.e. 3–5 kyr earlier than in core MD79257. Moreover, the second warming which follows the Antarctic Cold Reversal (ACR, Jouzel *et al*., 1995) leads by about 2 kyr the second SST increase at 20°S in the Indian Ocean. Finally, the temperature optimum in Antarctica is reached at about 9–10 cal kyr BP, i.e. 3 kyr before the Holocene SST maximum record in core MD79257. The timing of the deglaciation record at 20°S is thus compatible with the view that the break in climate synchroneity was at the Antarctic convergence instead of at the equator (Broecker, 1996).

Figure 8c shows the variations of the total abundance of C37 alkenones in core MD79257 ranging between 0.5 and 2.5 μg per gram of dry sediment. The core MD79257 being accurately dated, it is possible to evaluate accumulation rates. Unfortunately, the dry bulk density is not available for this core and, as a very crude approximation, we assumed that this parameter is constant with depth. In any case, the alkenone accumulation record (Fig. 11) is strongly dominated by the dramatic maximum of sedimentation rate dated at about 8 cal kyr BP which has been attributed to detrital input from the Zambezi river.

Fingerprinting of alkenone producers

The ratio of total C37 alkenones over the total of C38 alkenones (∑C37/∑C38) has been proposed to discriminate between the main alkenone producers, in particular between *E. huxleyi* and *G. oceanica* (Rosell-Melé *et al*., 1994; Volkman *et al*., 1995). Indeed, Volkman *et al*. (1995) and Sawada *et al*. (1996) found that the ∑C37/∑C38 ratios of *G. oceanica* are in general lower than those of *E. huxleyi*. However, Conte *et al*. (1997) recently found similar ∑C37/∑C38 ratios for different strains of both genus and suggested that the differences previously observed reflect rather

TABLE 4. Age and alkenone data for core MD79257 (20°24′S, 36°20′E, depth: 1262 m)

Deapath (cm)	Age cal-Kyr	C37 total μg g^{-1}	Σ37/38	$U^{K'}_{37}$	SST (°C)
0	1.2	0.80	1.01	0.952	26.8
4	1.5	1.33	1.13	0.954	26.9
10	2.1	1.37	1.15	0.954	26.9
32	3.8	0.46	1.07	0.965	27.2
40	4.3	0.40	1.06	0.969	27.4
48	4.7	0.48	1.17	0.963	27.2
59	5.3	0.50	1.22	0.961	27.1
68	5.7	0.58	1.21	0.961	27.1
78	6.1	0.53	1.20	0.967	27.3
87	6.4	0.40	1.01	0.970	27.4
99	6.7	0.49	1.07	0.974	27.5
112	7.1	0.62	1.09	0.975	27.5
118	7.2	1.10	1.23	0.951	26.8
130	7.4	0.60	1.20	0.965	27.2
190	7.9	1.26	1.81	0.944	26.6
199	8.0	1.26	1.26	0.941	26.5
210	8.0	1.86	1.23	0.941	26.5
215	8.0	1.03	1.16	0.943	26.6
226	8.1	0.96	1.23	0.938	26.5
230	8.1	1.71	1.21	0.938	26.4
239	8.1	1.15	1.18	0.943	26.6
250	8.2	1.23	1.17	0.951	26.8
260	8.3	1.32	1.60	0.945	26.7
270	8.5	0.93	1.21	0.949	26.8
280	8.7	1.15	1.19	0.952	26.8
289	8.9	0.82	1.19	0.952	26.9
299	9.2	0.70	1.19	0.952	26.9
310	9.4	1.13	1.30	0.926	26.1
320	9.6	1.12	1.28	0.933	26.3
329	9.8	0.66	1.32	0.933	26.3
339	10.1	0.98	1.26	0.926	26.1
343	10.2	0.98	1.30	0.938	26.4
353	10.4	0.97	1.31	0.932	26.3
358	10.5	0.81	1.30	0.931	26.2
369	10.7	0.76	1.24	0.926	26.1
382	10.9	0.82	1.31	0.936	26.4
392	11.0	0.68	1.26	0.934	26.3
398	11.1	0.68	1.31	0.938	26.4
411	11.3	0.53	1.25	0.930	26.2
414	11.4	0.60	1.22	0.934	26.3
420	11.5	1.23	1.26	0.923	26.0
435	11.7	0.97		0.917	25.8
445	11.9	0.70	1.23	0.920	25.9
452	12.0	0.42	1.11	0.917	25.8
462	12.2	0.63	1.25	0.916	25.8
472	12.4	0.53	1.25	0.925	26.1
482	12.6	0.87	1.20	0.924	26.0
492	12.8	0.68	1.67	0.921	25.9
502	13.1	0.66	1.29	0.922	26.0
512	13.4	0.37	0.57	0.925	26.1
523	13.8	0.40	1.33	0.925	26.1
534	14.3	0.59	1.06	0.926	26.1
544	14.7	0.71	1.25	0.928	26.1
554	15.2	0.53	1.16	0.919	25.9
564	15.7	0.48	1.36	0.885	24.9
574	16.3	0.37	1.09	0.878	24.7
584	16.9	0.89	1.10	0.875	24.6
591	17.4	0.96	1.17	0.901	25.4
601	18.0	0.87	1.17	0.876	24.6
613	18.9	0.93	1.16	0.891	25.0
622	19.6	1.33	1.28	0.863	24.2
633	20.4	1.36	1.42	0.890	25.0
641	20.7	1.50	1.33	0.899	25.3
651	21.2	1.05	1.16	0.901	25.4
662	21.8	1.08	1.17	0.892	25.1
672	22.3	0.76	1.18	0.898	25.3

TABLE 4. (Continued)

Deapath (cm)	Age cal-Kyr	C37 total $\mu g\,g^{-1}$	Σ37/38	$U^{K'}_{37}$	SST (°C)
682	22.9	0.62	1.10	0.899	25.3
692	23.4	0.97	1.17	0.897	25.2
702	23.9	1.36	1.19	0.902	25.4
714	24.6	1.19	1.17	0.910	25.6
721	25.0	1.30	1.13	0.898	25.3
731	25.5	1.30	1.17	0.920	25.9
741	26.0	1.18	1.14	0.917	25.8
751	26.6	1.71	1.20	0.924	26.0
761	27.1	1.21	1.12	0.917	25.8
771	27.6	0.87	1.07	0.892	25.1
781	28.2	1.20	1.24	0.900	25.3
792	28.7	1.05	1.12	0.910	25.6
802	29.3	1.46	1.18	0.917	25.8
812	29.8	1.59	1.13	0.190	25.6
822	30.3	0.64	1.24	0.907	25.5
831	30.8	2.40	1.16	0.921	25.9
841	31.3	0.98	1.17	0.912	25.7
851	31.9	0.94	1.22	0.909	25.6
861	32.4	0.87	1.22	0.922	26.0
871	32.9	1.21	1.16	0.899	25.3
881	33.5	1.00	1.16	0.903	25.4
891	34.0	0.93	1.19	0.929	26.2
901	34.6	0.60	1.16	0.925	26.1
911	35.2	0.79	1.18	0.932	26.3
921	35.8	0.99	1.23	0.913	25.7
931	36.4	0.97	1.14	0.908	25.6
941	37.0	1.32	1.20	0.915	25.8
951	37.6	1.43	1.18	0.920	25.9
961	38.3	1.67		0.910	25.6
971	39.0	2.10	1.23	0.914	25.7
981	39.7	0.84		0.916	25.8
991	40.5	0.52		0.931	26.2
1001	41.3	0.68	1.34	0.924	26.0
1011	42.1	2.45	1.20	0.941	26.5
1021	43.0	2.04	1.26	0.945	26.6
1031	43.9	1.88	1.26	0.947	26.7
1041	44.9	1.02	1.15	0.937	26.4

Note: C37 Total: C_{37} alkenone concentration (C37:3Me + C37:2Me) in μg per g of dry sediment; Σ37/38: (Total C37 alkenone)/ (total C38 alkenone); $U^{K'}_{37}$: unsaturation index for C37 alkenone, i.e. $[C_{37:2Me}]/([C_{37:3Me}] + [C_{37:2Me}])$; SST: sea surface temperature estimated using the equation: SST (°C) = $(U^{K'}_{37} - 0.039)/0.034$ of Prahl et al. (1988).

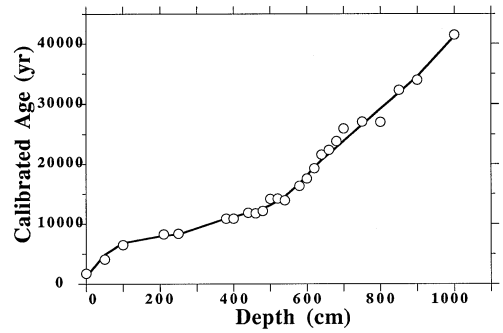

FIG. 9. Least-squares polynomial fitting of the age-depth relationship for the core MD79257 (Duplessy *et al.*, 1991). ^{14}C ages are corrected for reservoir age (400 yr) and calibrated into calendar ages by using U–Th ages in corals (Bard *et al.*, 1990, 1993). A flier at 950 cm has been discarded since it is 7 kyr younger than the surrounding sediment.

a difference in cell physiological state (log or stationary phase cultures) than a genetic difference between *E. huxleyi* and *G. oceanica.*

For the Arabian Sea core (MD 77194), the mean ∑C37/∑C38 is 1.21 (range 1.08–1.44, S.D. = 0.08, $n = 46$, Fig. 6d) for the last 25 kyr which roughly agrees with the ratios observed *E. huxleyi* cultures (Prahl *et al.*, 1988; mean = 1.46, S.D. = 0.21, range = 1.18–1.71, $n = 5$; Conte *et al.*, 1994, mean = 1.07, S.D. = 0.16, range = 0.86–1.40 and Sawada *et al.*, 1996, mean = 1.51; S.D. = 0.16, range = 1.30–1.87). The ∑C37/∑C38 ratios measured for the *G. oceanica* cultured by Volkman *et al.* (1995, mean = 0.70, S.D. = 0.08, range = 0.59–0.81, $n = 9$) are significantly different from those observed for the core MD77194. Nevertheless, *G. oceanica* is described as the dominant coccolith in the monsoon-influenced, northern and equatorial Indian Ocean (Prell *et al.*, 1980; Houghton and Guptha, 1991). This apparent discrepancy seems to confirm the culture results obtained by Conte *et al.* (1998).

For the southern Indian Ocean core (MD79257), the mean ∑C37/∑C38 is 1.21 (range = 0.57–1.81, S.D. = 0.13, $n = 102$, Fig. 8d) which is compatible with those of *E. huxleyi* cultures. These results are consistent with the study of coccoliths obtained on the same core (Beaufort, *pers. comm.*) and with analyses of the modern nannoplankton for this particular area (Friediner and Winter, 1987) confirming that *E. huxleyi* is the main alkenone producer at this site.

In addition, a mean ∑C37/∑C38 ratio of about 1.24 (S.D. 0.10, $n = 574$) is calculated by compiling all our measurements performed on late Quaternary sediments from the Indian Ocean. These results indicate that there is no obvious geographical pattern in the Indian Ocean and that the ∑C37/∑C38 ratio brings a limited information on the respective contribution of both producers in the Indian Ocean (Sonzogni *et al.*, 1997) as confirmed by Conte *et al.* (1998).

CONCLUSIONS

We have applied the alkenone method to a series of deep sea cores spread in the Indian Ocean. As studied in twenty cores, the tropics were about 1.5–2.5°C colder during the last glacial period. This conclusion agrees broadly paleotemperatures based on foraminifera distributions and $\delta^{18}O$ measured on individual foraminifera shells.

The last deglaciation at 10°N and 20°S is characterized by two warming steps which is similar to the classical deglacial chronology observed in the North Atlantic area. In particular, a small cold reversal corresponds to the Younger Dryas event.

At about 20°S, in the southern Indian Ocean the first deglacial warming is in phase (i.e. about 15 cal kyr BP) with northern hemisphere time series but significantly

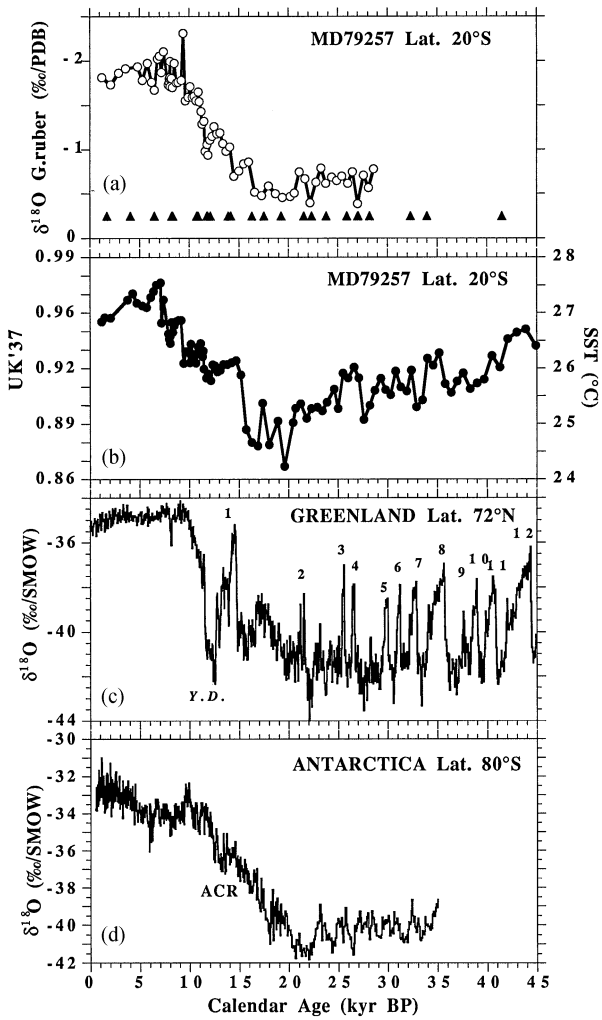

FIG. 10. (a) $\delta^{18}O$ time series for core MD79257 measured on the planktonic foraminifera *G. ruber* (Duplessy *et al.*, 1991; Caralp et al., 1993). Triangles indicate the age control points which are based on AMS-^{14}C dating of *G. ruber* (Duplessy *et al.*, 1991). The calendar time scale has been obtained by polynomial fitting through the calibrated AMS-^{14}C ages (see Fig. 9). (b) $U^{K'}_{37}$ time series for the last 45 kyr. SST have been calculated with the calibration by Prahl et al. (1988). The mid-point of the 1.5°C abrupt warming step occurs at the depth age level 559 cm (bracketed between $U^{K'}_{37}$ measurements at 554 and 564 cm). The nearest AMS-^{14}C ages are 11,900 $\pm$ 210 ^{14}C yr BP at 540 cm and 13,830 $\pm$ 230 ^{14}C yr BP at 580 cm which translate into calendar ages of $\approx$ 13,900 and $\approx$ 16,300 cal yr BP (Bard *et al.*, 1993). (c) $\delta^{18}O$ time series for the GRIP ice core from Greenland (Johnsen *et al.*, 1992) with an updated chronology (Hammer *et al.*, 1997). The numbering corresponds to interstadials, the so-called, Dansgaard–Oeschger events (Dansgaard *et al.*, 1993). Note the synchroneity between warm-cold oscillation in the marine core and the Dansgaard–Oeschger events 3, 4, 5, 6, 7, 8, 9, 11, 12. *YD*: Younger Dryas (see also Bard *et al.*, 1997). (d) $\delta^{18}O$ time series for the Byrd ice core (Johnsen *et al.*, 1972) with an updated chronology (Hammer *et al.*, 1994; Sowers and Bender, 1995). *ACR*: Antarctic Cold Reversal.

delayed with respect to Antarctica records (c.a. 18–20 cal kyr BP). This observation has several implications for understanding and modelling the atmospheric and oceanic links between the two hemispheres.

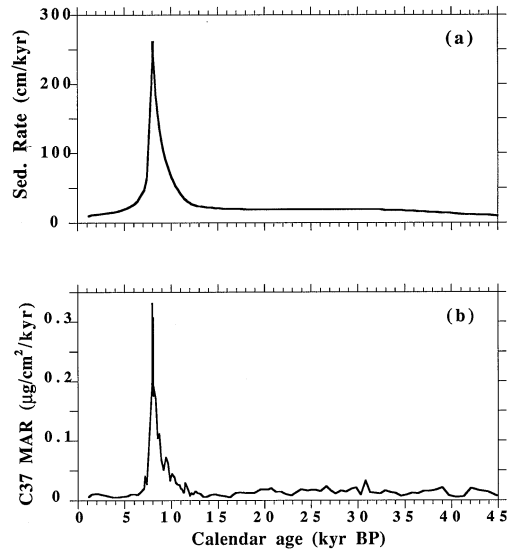

FIG. 11. (a) Sediment accumulation rate calculated from the age-depth record of core MD79257 shown in Fig. 9. (b) Mass accumulation rate (MAR) of C37 alkenones in core MD79257. A constant sediment density has been assumed as a first-order approximation.

ACKNOWLEDGMENTS

We are grateful to Dr J.P. Caulet and Dr J.C. Duplessy for giving access to cores stored at MNHN in Paris and CFR at Gif-sur-Yvette, respectively. We thank Dr L. Beaufort, Dr J.P. Caulet, Dr R. Schneider for useful discussions and Dr M. Arnold for help to construct an updated chronology for core MD79257. Isotopic data of ice cores from Greenland (GRIP) and Antarctica (Byrd) were kindly provided by Dr S. Johnsen. This study is supported by MENESR (JE192 and IUF) and PNEDC (INSU) and EC project TEMPUS.

REFERENCES

Alley, R.B., Meese, D.A., Shuman, C.A., Gow, A.J., Taylor, K.C., Grootes, P.M., White, J.W.C., Ram, M., Waddington, E.D, Mayewski, P.A. and Zielinski, G.A. (1993) Abrupt increase in Greenland snow accumulation at the end of the Younger Dryas event. *Nature*, **362**, 527–529.

Anderson, D.M. and Prell, W.L. (1993) A 300 kyr record of upwelling off Oman during the late Quaternary: Evidence of the Asian Southwest Monsoon. *Paleoceanography*, **8**, 193–208.

Anderson, D.M., Prell, W.L. and Barratt, N.J. (1989) Estimates of sea surface temperature in the coral sea at the last glacial maximum. *Paleoceanography*, **4**, 615–627.

Anderson, D.M. and Thunell, R.C. (1993) The oxygen-isotope composition of tropical ocean surface water during the last deglaciation. *Quaternary Science Reviews*, **12**, 465–473.

Bard, E., Arnold, M., Duprat, J., Moyes, J. and Duplessy, J.C. (1987) Retreat velocity of the North Atlantic polar front during the last deglaciation determinated by ^{14}C accelerator mass spectrometry. *Nature*, **328**, 791–794.

Bard, E., Arnold, M., Fairbanks, R.G. and Hamelin, B. (1993) ^{230}Th-^{234}U and ^{14}C ages obtained by mass spectrometry on corals. *Radiocarbon*, **35**, 191–199.

Bard, E., Hamelin, B., Fairbanks, R.G. and Zindler, A. (1990) Calibration of the ^{14}C timescale over the past 30,000 years using mass spectrometric U–Th ages from Barbados corals. *Nature*, **345**, 405–410.

Bard, E., Rostek, F. and Sonzogni, C. (1997) Interhemispheric synchrony of the last deglaciation inferred from the alkenone paleothermometry. *Nature*, **385**, 707–710.

Bassinot, F.C., Labeyrie, L.D., Vincent, E., Quidelleur, X., Shackleton, N.J. and Lancelot, Y. (1994) The astronomical theory of climate and the age of the Brunhes-Matuyama magnetic reversal. *Earth and Planetary Science Letters*, **126**, 91–108.

Beaufort, L., Lancelot, Y., Camberlain, P., Cayre, O., Vincent, E., Bassinot, F. and Labeyrie, L. (1997) Isolation cycels as a major control of equatorial Indian Ocean primary production. *Science*, **278**, 1451–1454.

Beck, J.W., Edwards, R.L., Ito, E., Taylor, F.W., Recy, J., Rougerie, F., Joannot, P. and Henin, C. (1992) Sea-surface temperature from coral skeletal Strontium/Calcium ratios. *Science*, **257**, 644–647.

Billups, K. and Spero, H.J. (1996) Reconstructing the stable isotope geochemistry and paleotemperatures of the equatorial Atlantic during the last 150,000 years: results from individual foraminifera. *Paleoceanography*, **11**, 217–238.

Bonnefille, R., Chalié, F., Guiot, J. and Vincens, A. (1992) Quantitative estimates of full glacial temperatures in equatorial Africa from palynological data. *Climate Dynamics*, **6**, 251–257.

Bonnefille, R., Roeland, J.C. and Guiot, J. (1990) Temperature and rainfall estimates for the past 40.000 years in equatorial Africa. *Nature*, **346**, 347–349.

Brassell, S.C., Eglinton, G., Marlowe, I.T., Pflaumann, U. and Sarnthein, M. (1986) Molecular stratigraphy: a new tool for climatic assessment. *Nature*, **320**, 129–133.

Broecker, W.S. (1986) Oxygen isotope constraints on surface ocean temperatures. *Quaternary Research*, **26**, 121–134.

Broecker, W.S. (1995) *The Glacial World According to Wally*, p. 318. Eldigio Press, Lamont-Doherty Earth Observatory of Columbia University, New-York.

Broecker, W.S. (1996) Paleoclimatology, *Geotimes*, **41**, 40–41.

Caralp, M.H., Duprat, J., Labeyrie, L. and Peypouquet (1993) Evolution paléohydrologique des eaux intermédiaires déduite d'une carotte d'âge quaternaire récent dans le canal de Mozambique. Apports des analyses isotopiques et microfauniques. *Bulletin de la Société Géologique de France*, **164**, 301–312.

Cayre, O. (1997a) Reconstitutions paléocéanographiques au Quaternaire récent à partir de l'analyse quantitative des foraminifères planctoniques dans l'Océan Indien et dans l'Atlantique Nord-Est. PhD Thesis. Université d'Aix-Marseille III.

Cayre, O., Beaufort, L. and Vincent, E. (1998) Paleoproductivity in the equatorial Indian Ocean for the last 260,000 yrs: a transfer function based on planktonic foraminifera. *Quaternary Science Reviews*. (in press).

Clemens, S., Prell, W., Murray, D., Shimmield, G. and Weedon, G. (1991) Forcing mechanisms in the Indian Ocean monsoon. *Nature*, **353**, 720–725.

CLIMAP Project Members (1981) Seasonal Reconstruction of the Earth's Surface at the Last Glacial Maximum. *Geological Society of America Map and Chart Series* MC–36.

Conte, M.H. and Eglinton, G. (1993) Alkenone and alkenoate distributions within the euphotic zone of the eastern North Atlantic: Correlation with production temperature. *Deep-Sea Research*, **40**, 1935–1962.

Conte, M.H., Thompson, A., Lesley, D. and Harris, R.P. (1997) Genetic and physiological influences on the alkenone/alkenoate versus growth temperature relationship in *Emiliania huxleyi* and *Gephyrocapsa oceanica*. *Geochimica Cosmochimica Acta* (in press).

Conte, M.H., Volkman, J.K. and Eglinton, G. (1994) Lipid biomarkers of the Prymnesiophyceae. *In*: Leadbeater, B.S.C. and Green, J.M. (eds.), *The Haptophyte Alga*, pp. 351–377. Oxford University Press, Oxford.

Crowley, T.J. and Matthews, R.K. (1983) Isotope-plankton comparisons in a late Quaternary core with a stable temperature history. *Geology*, **11**, 275–278.

Dansgaard, W., Johnsen, S.J., Clausen, H.B., Dahl-Jensen, D., Gundestrup, N.S., Hammer, C.U., Hvidberg, C.S., Steffensen, J.P., Sveinbjörnsdottir, A.E., Jouzel, J. and Bond, G. (1993) Evidence for general instability of past climate from a 250 kyr ice–core record. *Nature*, **364**, 218–220.

Duplessy, J.C. (1982) Glacial to interglacial contrasts in the northern Indian Ocean. *Nature*, **295**, 494–498.

Duplessy, J.C., Bard, E., Arnold, M., Shackleton, N.J., Duprat, J. and Labeyrie, L.D. (1991) How fast did the ocean-atmosphere system run during the last deglaciation? *Earth Planetary Science Letters*, **103**, 27–40.

Duplessy, J.C., Bé, A.W.H. and Blanc, P.L. (1981) Oxygen and carbon isotopic composition and biogeographic distribution of planktonic foraminifera in the Indian Ocean. *Paleogeography, Paleoclimatology, Paleoecology*, **33**, 9–46.

Eglinton, G., Bradshaw, S.A., Rosell, A., Sarnthein, M., Pflaumann, U. and Tiedmann, R. (1992) Molecular record of secular sea surface temperature changes on 100-year timescales for glacial terminations I, II and IV. *Nature*, **356**, 423–426.

Emeis, K.C., Anderson, D.M., Doose, H., Kroon, D. and Schulz-Bull, D. (1995a) Sea-Surface Temperatures and the History of the Monsoon Upwelling in the Northwest Arabian Sea during the Last 500,000 Years. *Quaternary Research*, **43**, 355–361.

Emeis, K.C., Doose, H., Mix, A. and Schulz-Bull, D. (1995b) Alkenone Sea-Surface Temperatures and Carbon burial at Site 846 (Eastern Equatorial Pacific Ocean): The Last Past 1.3 M.Y. In *Proceeding of the Ocean Drilling Program, Scientific Results*, **138**, 605–613.

Fairbanks, R.G. (1989) A 17,000-year glacio-eustatic sea level record: influence of glacial melting rates on the Younger Dryas event and deep-ocean circulation. *Nature*, **342**, 637–642.

Fontugne, M.R. and Duplessy, J.C. (1986) Variations of the monsoon regime during the upper Quaternary: evidence from carbon isotopic record of organic matter in North Indian Ocean sediment cores.*Paleogeography, Paleoclimatology, Paleoecology*, **56**, 69–88.

Friediner, P.J.J. and Winter, A. (1987) Distribution of modern coccolithophore assemblages in the southwest Indian Ocean off southern Africa. *Journal of Micropaleontology*, **6**, 49–56.

Ganssen, G., Troelstra, S.R. and van Weering, T. (1995) Younger Dryas, Younger Dryas style-event and the possible correlation with Heinrich events in deep-sea cores offshore Somalia (Indian Ocean) *In*: *The Younger Dryas*, Troelstra, S.R., van Hinte, J.E. and Ganssen G. (eds.), *Proceedings of a Workshop at the Royal Netherlands Academy of Arts and Sciences Kon.* Ned. Aka. van Wet., pp. 149–151.

Goslar, T., Arnold, M. Bard, E., Kuc, T., Pazdur, M.F., Ralska-Jasiewiczowa, M., Rozanski, K., Tisnerat, N., Walanus, A., Wicik, B. and Wieckowski, K. (1995) High concentration of atmospheric ^{14}C during the Younger Dryas cold episode. *Nature*, **377**, 414–417.

Guilderson, T.P., Fairbanks, R.G. and Rubenstone, J.L. (1994) Tropical temperature variations since 20,000 yrs ago: modulating interhemispheric climate change. *Science*, **263**, 663–665.

Hammer, C.U., Clausen, H.B. and Langway, C.C. (1994) Electrical conductivity method (ECM) stratigraphic dating of the Byrd Station ice core, Antarctica. *Annals of Glaciology*, **20**, 115–120.

Hammer, C.U. *et al.* (1997) The stratigraphic dating of the GRIP ice core. Niels Bohr Institute Rep. 1, (in press).

Herguera, J.C. and Berger, W.H. (1994) Glacial to postglacial drop in productivity in the western equatorial Pacific: Mixing rate vs. nutrient concentrations. *Geology*, **22**, 629–632.

Houghton, S.D. and Guptha, M.V.S. (1991) Monsoonal and fertility controls on recent marginal sea and continental shelf coccolith assemblages from the western Pacific and the northern Indian oceans. *Marine Geology*, **97**, 251–259.

Imbrie, J. and Kipp, N.G. (1971) A new micropaleontological method for paleoclimatology: application to a Late Pleistocene Caribbean core. *In*: Turekian, K.K. (ed.), *The Late Cenozoic Glacial Ages*, pp. 71–181. Yale Univ. Press, New Haven.

Johnsen, S.J., Dansgaard, W., Clausen, H.B. and Langway, C.C. (1972) Oxygen isotope profiles through the Antarctic and Greenland Ice sheets. *Nature*, **235**, 429–434.

Johnsen, S.J., Clausen, H.B., Dansgaard, W., Fuhrer, K., Gunderstrup, N., Hammer, C.U., Iversen, P., Jouzel, J., Stauffer, B. and Steffensen, J.P. (1992) Irregular glacial interstadials recorded in a new Greenland ice core. *Nature*, **359**, 311–313.

Jouzel, J., Vaikmae, R., Petit, J.R., Martin, M., Duclos, Y., Stievenard, M., Lorius, C., Toots, M., Mélières, M.A., Burckle, L.H., Barkov, N.I. and Kotlyakov, V.M. (1995) The two-step shape and timing of the last deglaciation in Antarctica. *Climate Dynamics*, **11**, 151–161.

Kallel, N. (1988) Variation de la composition isotopique de l'oxygène et du carbone des foraminifères: traceur de la circulation océanique pendant le dernier maximum glaciaire et lors de la dernière déglaciation. Ph D Thesis. Université Paris Sud-Orsay.

Levitus, S. (1994) World Ocean Atlas. NOAA Atlas NESDIS, U.S. Govt. Printing Office.

Linsley, B.K. (1996) Oxygen-isotope record of sea level and climate variations in the Sulu Sea over the past 150,000 years. *Nature*, **380**, 234–237.

Lyle, M., Prahl, F. and Sparrow, M. (1992) Upwelling and productivity changes inferred from a temperature record in the central equatorial Pacific, *Nature*, **355**, 812–815.

Miao, Q., Thunell, R.C. and Anderson, D.M. (1994) Glacial-Holocene carbonate dissolution and sea surface temperatures in the South China and Sulu seas. *Paleoceanography*, **9**, 269–290.

Min, G.R., Edwards, R.L., Taylor, F.W., Recy, J., Gallup, C.D. and Beck, J.W. (1995) Annual cycle of U/Ca in coral skeletons and U/Ca thermometry. *Geochimica Cosmochimica Acta*, **59**, 2025–2042.

Müller, P.J., Erlenkeuser, H. and von Grafenstein (1983) Glacial-interglacial cycles in oceanic productivity inferred from organic carbon contents in eastern North Atlantic sediment cores. *In*: Thiede, J. and Suess, E. (eds), *Coastal upwelling, its Sedimentary Record. Part B*: *sedimentary Records of Ancient Coastal Upwellings*. Plenum Press, New York.

Müller, P.J., Kirst, G., Ruhland, G., von Storch, I. and Rosell-Melé, A. (1997) Surface–sediment calibration of the alkenone unsaturation ratio $U^{K'}_{37}$ for paleotemperature estimation in the eastern South Atlantic Ocean. *Geochimica Cosmochimica Acta*, in press.

Ohkouchi, N., Kawamura, K., Nakamura, T. and Taira, A. (1994) Small changes in the Sea Surface Temperature during the last 20 000 years: molecular evidence from the western tropical Pacific. *Geophysical Research Letters*, **21**, 2207–2210.

Prahl, F.G., Muehlhausen, L.A. and Lyle, M. (1989) An organic geochimical assessment of oceanographic conditions at MANOP Site C over the Past 26,000 years. *Paleoceanography*, **4**, 495–510.

Prahl F.G., Muehlhausen, L.A. and Zahnle, D. (1988) Further evaluation of long-chain alkenones as indicators of paleoceanograpic conditions. *Geochimica Cosmochimica Acta*, **52**, 2303–2310.

Prahl, F.G., Pisias, N., Sparrow, M.A. and Sabin, A. (1995) Assessment of sea-surface temperature at 42°N in the California Current over the last 30,000 years. *Paleoceanography*, **10**, 763–773.

Prahl, F.G. and Wakeham, S.G. (1987) Calibration of unsaturation patterns in long-chain ketone compositions for palaeotemperature assessment. *Nature*, **330**, 367–369.

Prell, W.L. (1985) The stability of Low-Latitude Sea-Surface Temperatures: An Evaluation of the CLIMAP Reconstruction with Emphasis on the Positive SST Anomalies. Technical Report. TR025, United States Dept. of Energy, Washington, DC.

Prell, W.L., Hutson, W.H., Williams, D.F., Bé, A.W.H., Geitzenauer, K. and Molfino, B. (1980) Surface circulation of the Indian Ocean during the Last Glacial Maximum, approximatively 18,000 yr B.P. *Quaternary Research*, **14**, 309–336.

Prell, W.L. and Kutzbatch, J.E. (1987) Monsoon variability over the past 150,000 years. *Journal of Geophysical Research*, **92**, 8411–8425.

Rind, D. and Peteet, D. (1985) Terrestrial conditions at the Last Glacial Maximum and CLIMAP Sea-Surface-Temperature Estimates: Are They Consistent? *Quaternary Research*, **24**, 1–22.

Rosell-Melé, A., Carter, J. and Eglinton, G. (1994) Distribution of long-chain alkenones and alkyl alkenoates in marine sediments from the North East Atlantic. *Organic Geochemistry*, **22**, 501–509.

Rosell-Melé, A., Eglinton, G., Pflaumann, U. and Sarnthein, M. (1995) Atlantic core-top calibration of the Uk37 index as sea-surface paleotemperature indicator. *Geochimica Cosmochimica Acta*, **59**, 3099–3107.

Rostek F., Bard, E., Beaufort, L., Sonzogni, C. and Ganssen, G. (1997) Sea Surface Temperature and Productivity records for the past 240 kyr in the Arabian Sea. *Deep-Sea Research II*, **44**, 1461–1480.

Rostek, F., Ruhland, G., Bassinot, F.C., Beaufort, L., Müller, P.J. and Bard, E. (1994) Fluctuations of the Indian monsoon regime during the last 170,000 years: evidence from sea surface temperature, salinity and organic carbon records. *In*: Desbois, M. and Désalmand, F. (eds.), *Global Precipitations and Climate Change*, pp. 27–51, NATO ASI Series, vol. **I 26**. Springer, Heidelberg.

Rostek, F., Ruhland, G., Bassinot, F.C., Muller, P.J., Labeyrie, L.D., Lancelot, Y. and Bard, E. (1993) Reconstructing Sea Surface Temperature and Salinity using $\delta^{18}O$ and alkenone records. *Nature*, **364**, 319–321.

Sawada, K., Handa, N., Shiraiwa, Y., Dandara,A. and Montani,S. (1996) Long-chain alkenones and alkyl alkenoates in the coastal and pelagic sediments in the northwest North Pacific, with special reference to the reconstruction of *Emiliania huxleyi* and *Gephyrocapsa oceanica* ratios. *Organic Geochemistry*, **24**, 751–764.

Schrag, D.P., Hampt, G. and Murray, D.W. (1996) Pore fluid constraints on the temperature and oxygen isotopic composition of the Glacial Ocean. *Science*, **272**, 1930–1932.

Schneider, R., Müller, P.J. and Ruhland, G. (1995) Late Quaternary surface circulation in the east equatorial South Atlantic: Evidence from alkenone sea surface temperature. *Paleoceanography*, **10**, 197–220.

Sikes, E.L., Farrington, J.W. and Keigwin, L.D. (1991) Use of alkenone unsaturation ratio Uk37 to determine past sea surface temperatures: core-top SST calibrations and methodology considerations. *Earth and Planetary Science Letters*, **104**, 34–47.

Sikes, E.L. and Keigwin, L.D. (1994) Equatorial Atlantic Sea Surface Temperature for the last 30 kyr: a comparison of $U^{K'}_{37}$, $\delta^{18}O$ and foraminifera assemblage temperature estimates. *Paleoceanography*, **9**, 31–45.

Sikes, E.L. and Volkman, J.K. (1993) Calibration of long-chain alkenone unsaturation ratios for palaeotemperature estimation in cold polar waters. *Geochimica Cosmochimica Acta*, **57**, 1883–1889.

Sirocko, F., Sarnthein, M., Erlenkeuser, H., Lange, H., Arnold, M. and Duplessy, J.C. (1993) Century-scale events in monsoonal climate over the past 24,000 years. *Nature*, **364**, 322–324.

Sonzogni, C., Bard, E., Rostek, F., Dollfus, D., Rosell-Melé, A. and Eglinton, G. (1997) Temperature and salinity effects on alkenone ratios measured in surface sediments from the Indian Ocean. *Quaternary Research*, **47**, 344–355.

Sowers, T. and Bender, M. (1995) Climate records covering the last deglaciation, *Science*, **269**, 210–214.

Stott, L.D. and Tang, C.M. (1996) Reassessment of foraminiferal-based tropical sea surface $\delta^{18}O$ paleotemperatures. *Paleoceanography*, **11**, 37–56.

Stute, M., Forster, M., Frischkorn, H., Serejo, A., Clark, J.F., Schlosser, P., Broecker, W.S. and Bonani, G. (1994) Cooling of tropical Brazil (5°C) during the last glacial maximum. *Science*, **269**, 379–383.

Thompson, L.G., Mosley-Thompson, E., Davis, M.E., Lin, P.N., Henderson, K.A., Cole-Dai, J., Bolzan, J.F. and Liu, K.B. (1995) Late glacial stage and Holocene tropical ice core records from Huascaran, Peru. *Science*, **269**, 46–50.

Thunnel, R.C., Anderson, D., Gellar, D. and Miao, Q. (1994) Sea-surface temperature estimates for the tropical western Pacific during the Last Glaciation and their implications for the Pacific warm pool. *Quaternary Research*, **41**, 255–264.

Uerpmann, H.P. (1991) Radiocarbon dating of shell middens in the Sultanate of Oman. *PACT*, **29**, -IV.5, 335–347.

Van Campo, E., Duplessy, J.C., Prell, W.L., Barratt, N. and Sabatier, R. (1990) Comparison of terrestrial and marine temperatures estimates for the past 135 kyr off southeast Africa: a test for GCM simulations of paleoclimate. *Nature*, **348**, 209–212.

van Weering, T., Helder, W. and Schalk, P. (1997) The Netherlands Indian Ocean Expedition 1992–1993; first results and an introduction, *Deep-Sea Research II*, **44**, 1177–1193.

Vénec-Peyré, M.T., Caulet, J.P. and Vergnaud-Grazzini, C. (1995) Paleohydrographic changes in the Somali basin (5°N upwelling and equatorial areas) during the last 160 kyr, based on correspondence analysis of foraminiferal and radiolarian assemblages. *Paleoceanography*, **10**, 473–491.

Vergnaud-Grazzini, C., Caulet, J.P. and Vénec-Peyré, M.T. (1995) Index de fertilité et mousson dans le bassin de Somalie. Evolution au Quaternaire supérieur. *Bulletin de la Société Géologique de France*, **166**, 259–270.

Vincens, A. (1989) Les forêts claires zambéziennes du bassin Sud-Tanganyika. Evolution entre 25000 et 6000 ans B.P. *Compte Rendu de l'Académie des Sciences*, *Paris*, **308**, 809–814.

Volkman, J.K., Barrett, S.M., Blackburn, S.I. and Sikes, E.L. (1995) Alkenones in *Gephyrocapsa oceanica*; implications for studies of paleoclimate. *Geochimica Cosmochimica Acta*, **59**, 513–520.

Webster, P. and Streten N. (1978) Late Quaternary ice age climates of tropical Australasia, interpretation and reconstruction. *Quaternary Research*, **10**, 279–309.

Zhao, M., Rosell, A. and Eglinton, G. (1993) Comparison of two $U^{K'}_{37}$ sea surface temperature records for the last climatic cycle at ODP site 658 from the sub-tropical Northeast Atlantic. *Paleogeography Paleoclimatology Paleoecology*, **103**, 57–65.

Zhao, M., Beveridge, N.A.S., Shackleton, N.J., Sarnthein, M. and Eglinton, G. (1995) Molecular stratigraphy of cores off northwest Africa: Sea Surface Temperature history over the last 80 ka. *Paleoceanography*, **10**, 661–675.